Cholesky realized stochastic volatility model

Shinichiro Shirota [a,*], Yasuhiro Omori [b], Hedibert. F. Lopes [c], Haixiang Piao [d]

[a] Department of Statistical Science, Duke University, USA
[b] Faculty of Economics, The University of Tokyo, Japan
[c] Insper Institute of Education and Research, Brazil
[d] Nippon Life Insurance Company, Japan

ABSTRACT

Multivariate stochastic volatility models with leverage are expected to play important roles in financial applications such as asset allocation and risk management. However, these models suffer from two major difficulties: (1) there are too many parameters to estimate by using only daily asset returns and (2) estimated covariance matrices are not guaranteed to be positive definite. Our approach takes advantage of realized covariances to achieve the efficient estimation of parameters by incorporating additional information for the co-volatilities, and considers Cholesky decomposition to guarantee the positive definiteness of the covariance matrices. In this framework, a flexible model is proposed for stylized facts of financial markets, such as dynamic correlations and leverage effects among volatilities. By using the Bayesian approach, Markov Chain Monte Carlo implementation is described with a simple but efficient sampling scheme. Our model is applied to the data of nine U.S. stock returns, and it is compared with other models on the basis of portfolio performances.

© 2016 ECOSTA ECONOMETRICS AND STATISTICS. Published by Elsevier B.V. All rights reserved.

1. Introduction

Modeling time-varying co-volatilities of multiple asset returns has become increasingly important in recent years for financial risk management. Although there is considerable literature on univariate volatility models such as GARCH and stochastic volatility (SV) models, their extension to multivariate models has not been straightforward. The major concern in this field is the flexible and intuitive modeling of time-varying variances and correlations, but these multivariate volatility models suffer from two major difficulties: (1) there are too many parameters to estimate by using only daily asset returns and (2) estimated covariance matrices are not guaranteed to be positive definite. This paper proposes a promising solution to overcome these problems for a multivariate SV model by using a Cholesky decomposition of the covariance matrices and additional information of realized covariances.

Among multivariate SV models, factor models are intuitive to describe the high dimensional asset returns with common volatility dynamics and have been successful in reducing the number of parameters to estimate (Aguilar and West, 2000; Chib et al., 2006; Harvey et al., 1994; Pitt and Shephard, 2003) and Lopes and Carvalho (2007). However, we have to decide the number of factors a priori and choose the factor structure for parameter identification (Aguilar and West, 2000; Geweke and Zhou, 1996; Lopes and West, 2004). For more flexible modeling, this paper considers Cholesky decomposition of the covariance matrices, which guarantees the positive definiteness.

---

* Corresponding author. Fax: +81358415516.
  E-mail addresses: ss571@stat.duke.edu (S. Shirota), omori@e.u-tokyo.ac.jp (Y. Omori), hedibertFL@insper.edu.br (Hedibert. F. Lopes).

The Cholesky stochastic volatility (CSV) models introduce the dynamic structure to the diagonal and off-diagonal components of Cholesky-decomposed covariance matrices. Pourahmadi (1999) proposed to model components of (time-invariant) Cholesky-decomposed inverse covariance matrices as a linear function of predictors, and Fox and Dunson (2015) proposed a Bayesian nonparametric approach for the covariance regression. For the time-varying covariance structure, Lopes et al. (2014) considered the CSV model that incorporates dynamic structures to each diagonal and off-diagonal components of Cholesky-decomposed covariance matrices. This approach enables us to utilize parallel computing methods because of the conditional independence property of each row of decomposed components; thus it is efficient and fast even in high dimensional cases. In the class of GARCH models (see e.g., Bauwens et al., 2006 for a recent survey), Dellaportas and Pourahmadi (2012) proposed the Cholesky–GARCH model where conditional variances are assumed to follow the GARCH(1,1) process, but the nondiagonal elements of the lower triangular matrix of Cholesky decomposition are constant over time.

Furthermore, high-frequency (intraday) data of asset prices have become available recently in the financial market, and various realized measures have been proposed to estimate daily volatilities, which attracts attention in financial econometrics. These realized measures are, for example, realized volatility, realized kernel and realized covariance (Andersen and Bollerslev, 1998; Barndorff-Nielsen et al., 2008; Barndorff-Nielsen and Shephard, 2001) and Barndorff-Nielsen and Shephard (2004). These measures have more information regarding true volatilities or covariance matrices than those estimators based solely on daily returns, but they also have some biases primarily due to market microstructure noises and nontrading hours. To adjust these biases in SV models, realized stochastic volatility (RSV) models are proposed by Takahashi et al. (2009) where they consider simultaneous modeling of daily returns and realized volatilities, since daily returns are less subject to these biases. Compared to conventional SV models based solely on daily returns, the RSV models are expected to provide more accurate estimates of volatilities while removing biases of realized measures.

Several econometric models for realized covariances have been proposed in the literature. Jin and Maheu (2013), Jin and Maheu (2016) incorporated the realized covariance information into Wishart Autoregressive processes by extending models of Philipov and Glickman (2006) and Asai and McAleer (2009). Windle and Carvalho (2014) proposed a state space model whose observations and latent states take values on the manifold of symmetric positive-definite matrices, and Liu and Maheu (2015) jointly estimated returns and realized variances and covariances for Markov switching models. This paper considers multivariate RSV models in the context of CSV models. We incorporate realized covariances into the CSV models as additional information resources for true covariance matrices. Furthermore, we extend these original models to incorporate the dynamic leverage effects and correlations among volatilities. In empirical studies of nine U.S. stock returns, we compare our proposed model with standard CSV models on the basis of portfolio performances with several strategies.

The paper is organized as follows. Section 2 introduces the CSV and RSV models. In Section 3, we describe the Bayesian estimation procedure using Markov chain Monte Carlo (MCMC) simulation. We also discuss prior specifications for each parameters. Section 4 illustrates our estimation algorithm using simulated data. In Section 5, we apply our model to the data of nine U.S. stock returns data and show the empirical estimation results. Finally, in Section 6, we compare the performances of the proposed models with those of standard CSV models and simple benchmark models based on the basis of the different types of portfolio strategies.

2. Cholesky realized stochastic volatility model

In this section we introduce our Cholesky-realized SV (CRSV) model. We start by briefly reviewing (Lopes et al., 2014) the CSV model and Barndorff-Nielsen et al. (2011) the multivariate realized SV (RSV) model. These models tackle the two major difficulties in modeling multivariate volatility: positive-definiteness of estimated covariance matrices and the curse of dimensionality when estimating highly parameterized models for daily asset returns.

2.1. Cholesky stochastic volatility model

The Cholesky decomposition is unique and guarantees positive-definiteness of the covariance matrix when the diagonal components of the decomposed covariance are positive. More specifically, let $\mathbf{y}_t = (y_{1t}, \ldots, y_{pt})'$ be a p-dimensional vector of assets returns, such that

$$\mathbf{y}_t \sim \mathcal{N}(\mathbf{m}_t, \boldsymbol{\Sigma}_t) \tag{1}$$

where $\mathbf{m}_t = (m_{1t}, \ldots, m_{pt})'$ and $\boldsymbol{\Sigma}_t$ are the mean vector and the covariance matrix at time t, respectively. We consider the Cholesky decomposition of $\boldsymbol{\Sigma}_t$ for $t = 1, \ldots, n$ as follows:

$$\boldsymbol{\Sigma}_t = \mathbf{H}_t^{*-1} \mathbf{V}_t \mathbf{H}_t^{*-1'}, \tag{2}$$

where $\mathbf{V}_t = \text{diag}\{\exp(h_{11,t}), \ldots, \exp(h_{pp,t})\}$ and

$$\mathbf{H}_t^* = \begin{pmatrix} 1 & 0 & 0 & \ldots & 0 \\ -h_{21,t} & 1 & 0 & \ldots & 0 \\ -h_{31,t} & -h_{32,t} & 1 & \ddots & \vdots \\ \vdots & \vdots & \ddots & \ddots & 0 \\ -h_{p1,t} & -h_{p2,t} & \ldots & -h_{p\,p-1,t} & 1 \end{pmatrix}, \tag{3}$$

Recursive conditional regressions. It follows that

$$\mathbf{H}_t^*(\mathbf{y}_t - \mathbf{m}_t) \sim \mathcal{N}(\mathbf{0}, \mathbf{V}_t),$$

where the quantities $h_{ij,t}$'s $(i > j)$ are the regression coefficients in p recursive conditional regressions:

$$y_{it}\big|\{y_{jt}\}_{j=1}^{i-1} \sim \mathcal{N}\left(m_{i,t} + \sum_{j=1}^{i-1} h_{ij,t}(y_{jt} - m_{jt}), \ \exp(h_{ii,t})\right), \quad i = 1, \dots, p.$$

Lopes et al. (2014) proposed the CSV models by assuming $\mathbf{m}_t = \mathbf{0}$ and autoregressive processes for $\mathbf{h}_t = (h_{11,t}, h_{22,t}, \dots, h_{pp,t})'$ and $\mathbf{h}_t^* = (h_{21,t}, h_{31,t}, \dots, h_{p\,p-1,t})'$,

$$\mathbf{h}_{t+1} = \boldsymbol{\mu} + \boldsymbol{\Phi}(\mathbf{h}_t - \boldsymbol{\mu}) + \boldsymbol{\eta}_t, \quad \boldsymbol{\eta}_t \sim \text{ i.i.d. } \mathcal{N}(\mathbf{0}, \mathbf{D}), \tag{4}$$

$$\mathbf{h}_{t+1}^* = \boldsymbol{\mu}^* + \boldsymbol{\Phi}^*(\mathbf{h}_t^* - \boldsymbol{\mu}^*) + \boldsymbol{\eta}_t^*, \quad \boldsymbol{\eta}_t^* \sim \text{ i.i.d. } \mathcal{N}(\mathbf{0}, \mathbf{D}^*), \tag{5}$$

where $\boldsymbol{\mu} = (\mu_{11}, \mu_{22}, \dots, \mu_{pp})'$, $\boldsymbol{\mu}^* = (\mu_{21}, \mu_{31}, \dots, \mu_{p\,p-1})'$, $\boldsymbol{\Phi} = \text{diag}(\boldsymbol{\phi})$, $\boldsymbol{\phi} = (\phi_{11}, \phi_{22}, \dots, \phi_{pp})'$, $\boldsymbol{\Phi}^* = \text{diag}(\boldsymbol{\phi}^*)$, $\boldsymbol{\phi}^* = (\phi_{21}, \phi_{31}, \dots, \phi_{p\,p-1})'$, $\mathbf{D} = \text{diag}(\tau_{11}^2, \tau_{22}^2, \dots, \tau_{pp}^2)$, and $\mathbf{D}^* = \text{diag}(\tau_{21}^2, \tau_{31}^2, \dots, \tau_{p\,p-1}^2)$. They implement the highly efficient estimation based on the mixture sampler (see, Kim et al., 1998 and Omori et al., 2007) by using the normal mixture approximation. The CSV model enables us to utilize parallel computing procedures for estimating each component because of the conditional independence of each row.

2.2. Realized stochastic volatility model

Another major difficulty in the multivariate volatility model is that there are too many parameters to estimate by using only daily asset returns. In addition to daily returns, recently, high frequency datasets have become available and have attracted attention in financial econometrics. By using high frequency data, Andersen and Bollerslev (1998) and Barndorff-Nielsen and Shephard (2002) proposed a more accurate volatility estimator termed the realized volatility. However, in the presence of the market microstructure noises, it becomes a biased estimator and Barndorff-Nielsen et al. (2008) further proposed the realized kernel, which is a robust estimator to such noises. Several other extensions of these estimators have been proposed under different assumptions for the stochastic processes of assets. For multivariate asset returns, the realized covariance, $\mathbf{RC}_t$, is defined by

$$\mathbf{RC}_t = \sum_{j=1}^{m} \mathbf{r}_{j,t}\mathbf{r}_{j,t}',$$

where $\mathbf{r}_{j,t} = \mathbf{y}_{\frac{j}{m},t} - \mathbf{y}_{\frac{j-1}{m},t}$, $j = 1, \dots, m$, $t = 1, \dots, n$, and $\mathbf{y}_{\frac{j}{m},t}$ is a $p \times 1$ log-price vector at j-th time of the day t. Barndorff-Nielsen and Shephard (2004) show that, in the absence of the market microstructure noise, it converges to the quadratic covariation of $\mathbf{y}_t$ as $m \to \infty$. Barndorff-Nielsen et al. (2011) proposed the multivariate realized kernel that is robust to such noises. Although various extensions of these estimators have been proposed, their properties depend on assumptions imposed on the price processes.

The realized measures have more information regarding true volatilities and covariance matrices, while there may be a bias due to the market microstructure noise. Furthermore, daily returns have less information about true volatilities, while they are less affected by these noises. Thus (Takahashi et al., 2009) proposed RSV models, which involve the simultaneous modeling of daily returns and realized volatilities, there is a growing literature on similar simultaneous modeling (Koopman and Scharth, 2013; Shirota et al., 2014; Venter and de Jongh, 2014) and Zheng and Song (2014). In addition to the standard stochastic volatility model with leverage

$$y_t = \exp\{h_t/2\}\epsilon_t, \tag{6}$$

$$h_{t+1} = \mu + \phi(h_t - \mu) + \eta_t, \tag{7}$$

for $t = 1, \dots, n$ and

$$\begin{pmatrix} \epsilon_t \\ \eta_t \end{pmatrix} \sim \text{ i.i.d. } \mathcal{N}\left(\begin{pmatrix} 0 \\ 0 \end{pmatrix}, \begin{pmatrix} 1 & \rho\sigma_\eta \\ \rho\sigma_\eta & \sigma_\eta^2 \end{pmatrix}\right), \tag{8}$$

where y_t is an asset returns at time t, Takahashi et al. (2009) consider another measurement equation for the logarithm of the realized volatility at time t

$$x_t = \xi + h_t + u_t, \tag{9}$$

where $u_t \sim \text{ i.i.d. } \mathcal{N}(0, \sigma_u^2)$ and is independent of $(\epsilon_t, \eta_t)'$. This model automatically adjusts the bias of the realized measure without any additional adjustment such as selecting the optimal sampling frequency to compute the realized volatility. The parameter ξ is the bias adjustment term to account for the effects of the market microstructure noise and nontrading

hours simultaneously. When it is negative (positive), the realized volatility is considered to underestimate (overestimate) the latent volatility. Although we could extend this parameter by replacing h_t with ψh_t in (9), where ψ is another adjustment coefficient, it has been pointed out that this extension does not necessarily improve the forecasting performances in the empirical studies.

2.3. Cholesky realized stochastic volatility model with leverage

We now extend the CSV model in two directions. First, we consider additional measurement equations to incorporate the information of the realized measures. Second, we incorporate leverage effects that are often observed to exist in the empirical studies of stock markets.

Consider the Cholesky decomposition of the realized covariance $\mathbf{RC}_t$ given by

$$\mathbf{RC}_t = \mathbf{X}_t^{*-1} \, \mathrm{diag}\{\exp(x_{11,t}), \exp(x_{22,t}), \ldots, \exp(x_{pp,t})\} \, \mathbf{X}_t^{*-1'},$$

where

$$\mathbf{X}_t^* = \begin{pmatrix} 1 & 0 & 0 & \cdots & 0 \\ -x_{21,t} & 1 & 0 & \cdots & 0 \\ -x_{31,t} & -x_{32,t} & 1 & \ddots & \vdots \\ \vdots & \vdots & \ddots & \ddots & 0 \\ -x_{p1,t} & -x_{p2,t} & \cdots & -x_{p\,p-1,t} & 1 \end{pmatrix},$$

and defining $\boldsymbol{x}_t = (x_{11,t}, x_{22,t}, \ldots, x_{pp,t})'$ and $\boldsymbol{x}_t^* = (x_{21,t}^*, x_{31,t}^*, \ldots, x_{p\,p-1,t}^*)'$. The information of the realized covariances is added to the following measurement equations:

$$\boldsymbol{x}_t = \boldsymbol{\xi} + \boldsymbol{h}_t + \boldsymbol{u}_t, \quad \boldsymbol{u}_t \sim \text{i.i.d.} \ \mathcal{N}(\mathbf{0}, \mathbf{C}), \tag{10}$$

$$\boldsymbol{x}_t^* = \boldsymbol{\xi}^* + \boldsymbol{h}_t^* + \boldsymbol{u}_t^*, \quad \boldsymbol{u}_t^* \sim \text{i.i.d.} \ \mathcal{N}(\mathbf{0}, \mathbf{C}^*), \tag{11}$$

where $\boldsymbol{\xi} = (\xi_{11}, \xi_{22}, \ldots, \xi_{pp})'$, $\boldsymbol{\xi}^* = (\xi_{21}, \xi_{31}, \ldots, \xi_{p\,p-1})'$, $\mathbf{C} = \mathrm{diag}(\sigma_{u,11}^2, \sigma_{u,22}^2, \ldots, \sigma_{u,pp}^2)'$, and $\mathbf{C}^* = \mathrm{diag}(\sigma_{u,21}^2, \sigma_{u,31}^2, \ldots, \sigma_{u,p\,p-1}^2)'$.

The $\boldsymbol{u}_t$ and $\boldsymbol{u}_t^*$ are the measurement error terms for realized covariances, which are assumed to be independent of each other. Further, we assume the common bias ξ for realized covariances, i.e., $\boldsymbol{\xi} = \xi \mathbf{1}_p$ where $\mathbf{1}_p$ is a $p \times 1$ vector with all elements equal to one so that

$$\mathbf{RC}_t = \exp(\xi)\mathbf{X}_t^{*-1} \, \mathrm{diag}(\exp(h_{11,t} + u_{1t}), , \ldots, \exp(h_{pp,t} + u_{pt})) \, \mathbf{X}_t^{*-1'}.$$

In the model with leverage, there are many parameters to be estimated, and hence, some parameter estimates could become unstable. In such a case, the common bias assumption is helpful to reduce the number of parameters and to obtain stable parameter estimates. In fact, all asset returns are assumed to be observed simultaneously, and they are subject to common microstructure noises, nontrading hours, and so on, which indicates the bias caused by these problems is common to all realized variances and justifies the common ξ in (10). We note that the common scale bias $\exp(\xi)$ does not affect the correlation structure of realized covariances, while the bias adjustment terms for off-diagonal components $\boldsymbol{\xi}^*$ may affect the correlation structure of covariance matrices. We could consider additional bias adjustment coefficient matrices for $\boldsymbol{h}$ and $\boldsymbol{h}^*$, but assume that they are unit matrices for simplicity.

We now consider leverage and cross-leverage effects that are observed to exist in stock markets to improve the predictive performance of the model (e.g., Ishihara and Omori, 2012; Ishihara et al., 2016; Trojan, 2015). The cross-leverage effects are defined as the negative correlation between the ith asset return at time t and the jth log volatility at time $t + 1$ for $i \neq j$. Given $\boldsymbol{y}_t$, $\boldsymbol{h}_t$ and $\boldsymbol{m}_t$, we incorporate dynamic leverage effects through the following equations:

$$\boldsymbol{h}_{t+1} = \boldsymbol{\mu} + \boldsymbol{\Phi}(\boldsymbol{h}_t - \boldsymbol{\mu}) + \mathbf{RV}_t^{-1/2}\mathbf{H}_t^*(\boldsymbol{y}_t - \boldsymbol{m}_t) + \boldsymbol{\zeta}_t,$$

where $\boldsymbol{\zeta}_t \sim \mathcal{N}(\mathbf{0}, \boldsymbol{\Omega})$, with $\boldsymbol{\Omega} = \mathbf{S}^{-1}\mathbf{D}\mathbf{S}^{-1'}$ and

$$\mathbf{S} = \begin{pmatrix} 1 & 0 & 0 & \cdots & 0 \\ -s_{21} & 1 & 0 & \cdots & 0 \\ -s_{31} & -s_{32} & 1 & \ddots & \vdots \\ \vdots & \vdots & \ddots & \ddots & 0 \\ -s_{p1} & -s_{p2} & \cdots & -s_{p\,p-1} & 1 \end{pmatrix}.$$

The $p \times p$ matrix $\mathbf{R}$ captures the influence of daily returns at time t on the diagonal elements of covariance matrices at time $t + 1$. We could consider similar effects for h_{t+1}^*, but their interpretations are not clear in empirical studies. Moreover, these effects will introduce a large number of parameters (order p^4). Thus we focus on leverage effects only for $\boldsymbol{h}_{t+1}$. Further, the

matrix $\mathbf{S}$ describes the dependence among $\boldsymbol{h}_{t+1}$ in a sequential regression form. Since time-varying variances of multiple asset returns move in a similar direction in the financial market, we expect them to have high correlation and hence incorporate the correlation through the matrix $\mathbf{S}$. Setting $\mathbf{R} = \mathbf{O}$ and $\mathbf{S} = \mathbf{I}_p$ where $\mathbf{I}_p$ denotes a $p \times p$ identity matrix, it reduces to the model without leverage as reported in Lopes et al. (2014).

Finally, we assume a random walk process for the mean process of $\boldsymbol{y}_t$ to allow possible dynamic movement in mean levels rather than setting $\boldsymbol{m}_t \equiv \mathbf{0}$. We note that the introduction of such a mean process is important to improve the portfolio performance in empirical studies.

In summary, we propose the CRSV model given by three measurement equations

$$\boldsymbol{y}_t = \boldsymbol{m}_t + \mathbf{H}_t^{*-1} \mathbf{V}_t^{1/2} \boldsymbol{\epsilon}_t, \tag{12}$$

$$\boldsymbol{x}_t = \xi \mathbf{1}_p + \boldsymbol{h}_t + \boldsymbol{u}_t, \quad \boldsymbol{u}_t \sim \text{i.i.d. } \mathcal{N}(\mathbf{0}, \mathbf{C}), \tag{13}$$

$$\boldsymbol{x}_t^* = \boldsymbol{\xi}^* + \boldsymbol{h}_t^* + \boldsymbol{u}_t^*, \quad \boldsymbol{u}_t^* \sim \text{i.i.d. } \mathcal{N}(\mathbf{0}, \mathbf{C}^*), \tag{14}$$

for $t = 1, \ldots, n$ and three state equations

$$\boldsymbol{h}_{t+1} = \boldsymbol{\mu} + \boldsymbol{\Phi}(\boldsymbol{h}_t - \boldsymbol{\mu}) + \boldsymbol{\eta}_t, \tag{15}$$

$$\boldsymbol{h}_{t+1}^* = \boldsymbol{\mu}^* + \boldsymbol{\Phi}^*(\boldsymbol{h}_t^* - \boldsymbol{\mu}^*) + \boldsymbol{\eta}_t^*, \quad \boldsymbol{\eta}_t^* \sim \text{ i.i.d. } \mathcal{N}(\mathbf{0}, \mathbf{D}^*), \tag{16}$$

$$\boldsymbol{m}_{t+1} = \boldsymbol{m}_t + \boldsymbol{v}_t, \quad \boldsymbol{v}_t \sim \text{ i.i.d. } \mathcal{N}(\mathbf{0}, \boldsymbol{\Omega}_m), \quad \boldsymbol{\Omega}_m = \text{diag}(\sigma_{m1}^2, \ldots, \sigma_{mp}^2), \tag{17}$$

for $t = 1, \ldots, n-1$ where

$$\begin{pmatrix} \boldsymbol{\epsilon}_t \\ \boldsymbol{\eta}_t \end{pmatrix} \sim \text{ i.i.d. } \mathcal{N}\left(\mathbf{0}, \begin{pmatrix} \mathbf{I}_p & \mathbf{R}' \\ \mathbf{R} & \mathbf{RR}' + \mathbf{S}^{-1}\mathbf{DS}^{-1'} \end{pmatrix} \right).$$

For initial values of state variables, we assume, for simplicity,

$$\boldsymbol{h}_1 \sim \mathcal{N}(\boldsymbol{\mu}, \lambda \mathbf{S}^{-1}\mathbf{DS}^{-1'}), \quad \boldsymbol{h}_1^* \sim \mathcal{N}(\boldsymbol{\mu}^*, \lambda^* \mathbf{D}^*), \quad \boldsymbol{m}_1 \sim \mathcal{N}(\mathbf{0}^*, \lambda_m \boldsymbol{\Omega}_m),$$

where $\lambda, \lambda^*, \lambda_m$ are set to some known large constant.

3. Posterior inference

3.1. Prior distributions

We consider the vague prior distribution for each component of parameters if we do not have sufficient prior information on parameters. For example, we assume univariate normal distribution for ξ and independent multivariate normal distributions for $\boldsymbol{\xi}^*$, $\boldsymbol{\mu}$ and $\boldsymbol{\mu}^*$ with large variance. For the vectorized components of $\mathbf{S}$ and $\mathbf{R}$, we assume independent multivariate normal distribution with large variance. Furthermore, for the components of $\mathbf{C}$, $\mathbf{C}^*$, $\mathbf{D}$, $\mathbf{D}^*$ and $\boldsymbol{\Omega}_m$, we consider inverse gamma distribution with large variance for the conjugacy property. For the prior distribution for ϕ, we assume beta distribution for $(\phi + 1)/2$ that is often used in the previous empirical studies for the univariate models.

With regard to the prior distribution of ϕ^*, we need more careful discussion. Lopes et al. (2014) introduced variable selection priors for $\boldsymbol{\phi}^*$. This approach is flexible because it includes several dynamic patterns for $\boldsymbol{h}_t^*$ such as the constant plus noise and the random walk process. Since the constant plus noise process has an almost similar path to that of the random walk process with a small error variance, we consider the prior distribution for $\boldsymbol{\phi}^*$ to include random walk processes for $\boldsymbol{h}_t^*$. Noting that the random walk process is nonstationary with the unit root, we considered three types of unit root priors for $\boldsymbol{\phi}^*$ proposed in the literature: (1) the beta prior defined not on $(-1, 1)$, but on a slightly extended range so as to allow for slightly explosive values (Lubrano, 1995):

$$\pi(\phi_i^*) \propto (1 + \nu - \phi_i^{*2})^{-1/2}, \quad -\sqrt{1+\nu} < \phi_i^* < \sqrt{1+\nu},$$

where ν is a small positive number, (2) the reference prior (Berger and Yang, 1994) given by

$$\pi(\phi_i^*) = \begin{cases} \left(2\pi\sqrt{1 - \phi_i^{*2}}\right)^{-1}, & |\phi_i^*| < 1, \\ \left(2\pi|\phi_i^*|\sqrt{\phi_i^{*2} - 1}\right)^{-1}, & |\phi_i^*| \geq 1, \end{cases}$$

and (3) the uniform prior on $(-\sqrt{1+\nu}, \sqrt{1+\nu})$, $\phi_i^* \sim \mathcal{U}(-\sqrt{1+\nu}, \sqrt{1+\nu})$, by setting $\varphi = \frac{\sqrt{1+\nu}+\phi}{2\sqrt{1+\nu}} \sim \mathcal{B}(1, 1)$. In empirical studies, we take $\nu = 0.3$ since it is sufficient to cover the support of posterior probability density function of ϕ_i^*, and no differences are found in the sensitivity analysis for these three different prior settings. Thus, we focus on the simple uniform prior on $(-\sqrt{1+\nu}, \sqrt{1+\nu})$ with $\nu = 0.3$.

Since we include the realized covariance as an additional source of information of covariance matrices in CRSV models, the estimation of $\boldsymbol{\phi}^*$ is more stable and efficient than that in CSV models. However, the off-diagonal components of realized covariance are still noisy as shown in the empirical studies, and allowing for $\boldsymbol{h}_t^*$ to follow the smooth random walk process is more appropriate to estimate $\boldsymbol{\phi}_*$ rather than imposing the conventional stationarity conditions.

3.2. Customized MCMC scheme

By using the Bayesian approach, we implement an MCMC simulation and estimate posterior distributions of the parameters to conduct statistical inferences. Let $\boldsymbol{z} = \{\boldsymbol{y}, \boldsymbol{x}\}$ denote the set of observations where $\boldsymbol{y} = \{\boldsymbol{y}_1, \boldsymbol{y}_2, \ldots, \boldsymbol{y}_n\}$, $\boldsymbol{x} = \{\boldsymbol{x}_1, \boldsymbol{x}_2, \ldots, \boldsymbol{x}_n\}$, and $\boldsymbol{x}^* = \{\boldsymbol{x}_1^*, \boldsymbol{x}_2^*, \ldots, \boldsymbol{x}_n^*\}$. Further let $\boldsymbol{\theta}$ denote the set of parameters $\{\xi, \boldsymbol{\xi}^*, \boldsymbol{\mu}, \boldsymbol{\mu}^*, \boldsymbol{\phi}, \boldsymbol{\phi}^*, \mathbf{R}, \mathbf{S}, \mathbf{C}, \mathbf{C}^*, \mathbf{D},$ $\mathbf{D}^*, \boldsymbol{\Omega}_m\}$, and define the set of latent variables as $\boldsymbol{m} = \{\boldsymbol{m}_1, \boldsymbol{m}_2, \ldots, \boldsymbol{m}_n\}$, $\boldsymbol{h} = \{\boldsymbol{h}_1, \boldsymbol{h}_2, \ldots, \boldsymbol{h}_n\}$, and $\boldsymbol{h}^* = \{\boldsymbol{h}_1^*, \boldsymbol{h}_2^*, \ldots, \boldsymbol{h}_n^*\}$. We generate random samples from the posterior distribution with the probability density function $\pi(\boldsymbol{\theta}, \boldsymbol{m}, \boldsymbol{h}, \boldsymbol{h}^*|\boldsymbol{z})$ given by

$$
\begin{aligned}
\log \pi(\boldsymbol{\theta}, \boldsymbol{m}, \boldsymbol{h}, \boldsymbol{h}^*|\boldsymbol{z}) = {}& \text{const.} + \log \pi(\boldsymbol{\theta}) - \frac{1}{2}\sum_{t=1}^{n}\sum_{i=1}^{p} h_{ii,t} - \frac{n}{2}\sum_{i=1}^{p}\sum_{j=1}^{i}\log\sigma_{u,ij}^2 - \frac{n}{2}\sum_{i=1}^{p}\log\sigma_{mi}^2 - \frac{n}{2}\sum_{i=1}^{p}\sum_{j=1}^{i}\log\tau_{ij}^2 \\
& -\frac{1}{2}\sum_{t=1}^{n}(\boldsymbol{y}_t - \boldsymbol{m}_t)'\mathbf{H}_t^{*\prime}\mathbf{V}_t^{-1}\mathbf{H}_t^*(\boldsymbol{y}_t - \boldsymbol{m}_t) - \frac{1}{2}\sum_{t=1}^{n}(\boldsymbol{x}_t - \xi\mathbf{1}_p - \boldsymbol{h}_t)'\mathbf{C}^{-1}(\boldsymbol{x}_t - \xi\mathbf{1}_p - \boldsymbol{h}_t) \\
& -\frac{1}{2}\sum_{t=1}^{n}(\boldsymbol{x}_t^* - \boldsymbol{\xi}^* - \boldsymbol{h}_t^*)'\mathbf{C}^{*-1}(\boldsymbol{x}_t^* - \boldsymbol{\xi}^* - \boldsymbol{h}_t^*) - \frac{1}{2}\sum_{t=1}^{n}(\boldsymbol{m}_{t+1} - \boldsymbol{m}_t)'\boldsymbol{\Omega}_m^{-1}(\boldsymbol{m}_{t+1} - \boldsymbol{m}_t) \\
& -\frac{1}{2}\sum_{t=1}^{n-1}\{\boldsymbol{h}_{t+1} - \boldsymbol{\mu} - \boldsymbol{\Phi}(\boldsymbol{h}_t - \boldsymbol{\mu}) - \mathbf{R}\mathbf{V}_t^{-1/2}\mathbf{H}_t^*(\boldsymbol{y}_t - \boldsymbol{m}_t)\}'\mathbf{S}'\mathbf{D}^{-1}\mathbf{S} \\
& \qquad\qquad \{\boldsymbol{h}_{t+1} - \boldsymbol{\mu} - \boldsymbol{\Phi}(\boldsymbol{h}_t - \boldsymbol{\mu}) - \mathbf{R}\mathbf{V}_t^{-1/2}\mathbf{H}_t^*(\boldsymbol{y}_t - \boldsymbol{m}_t)\} \\
& -\frac{1}{2}\sum_{t=1}^{n-1}\{\boldsymbol{h}_{t+1}^* - \boldsymbol{\mu}^* - \boldsymbol{\Phi}^*(\boldsymbol{h}_t^* - \boldsymbol{\mu}^*)\}'\mathbf{D}^{*-1}\{\boldsymbol{h}_{t+1}^* - \boldsymbol{\mu}^* - \boldsymbol{\Phi}^*(\boldsymbol{h}_t^* - \boldsymbol{\mu}^*)\} \\
& -\frac{1}{2\lambda_m}\boldsymbol{m}_1'\boldsymbol{\Omega}^{-1}\boldsymbol{m}_1 - \frac{1}{2\lambda}(\boldsymbol{h}_1 - \boldsymbol{\mu})'\mathbf{S}'\mathbf{D}^{-1}\mathbf{S}(\boldsymbol{h}_1 - \boldsymbol{\mu}) - \frac{1}{2\lambda^*}(\boldsymbol{h}_1^* - \boldsymbol{\mu}^*)'\mathbf{D}^{*-1}(\boldsymbol{h}_1^* - \boldsymbol{\mu}^*),
\end{aligned}
\tag{18}
$$

where $\pi(\boldsymbol{\theta})$ denote the prior density function of $\boldsymbol{\theta}$.

The MCMC algorithm is implemented in ten blocks:

1. Initialize $\boldsymbol{\theta}$, $\boldsymbol{m}$, $\boldsymbol{h}$ and $\boldsymbol{h}^*$.
2. Generate $\boldsymbol{h}|\boldsymbol{\theta}, \boldsymbol{m}, \boldsymbol{h}^*, \boldsymbol{z}$
3. Generate $\boldsymbol{h}^*|\boldsymbol{\theta}, \boldsymbol{m}, \boldsymbol{h}, \boldsymbol{z}$
4. Generate $\boldsymbol{m}|\boldsymbol{\theta}, \boldsymbol{h}, \boldsymbol{h}^*, \boldsymbol{z}$
5. Generate $(\xi, \boldsymbol{\xi}^*, \boldsymbol{\mu}, \boldsymbol{\mu}^*)|\boldsymbol{\theta}_{\backslash(\xi, \boldsymbol{\xi}^*, \boldsymbol{\mu}, \boldsymbol{\mu}^*)}, \boldsymbol{m}, \boldsymbol{h}, \boldsymbol{h}^*, \boldsymbol{z}$
6. Generate $(\boldsymbol{\phi}, \boldsymbol{\phi}^*)|\boldsymbol{\theta}_{\backslash(\boldsymbol{\phi}, \boldsymbol{\phi}^*)}, \boldsymbol{m}, \boldsymbol{h}, \boldsymbol{h}^*, \boldsymbol{z}$
7. Generate $\mathbf{R}|\boldsymbol{\theta}_{\backslash\mathbf{R}}, \boldsymbol{m}, \boldsymbol{h}, \boldsymbol{h}^*, \boldsymbol{z}$
8. Generate $\mathbf{S}|\boldsymbol{\theta}_{\backslash\mathbf{S}}, \boldsymbol{m}, \boldsymbol{h}, \boldsymbol{h}^*, \boldsymbol{z}$
9. Generate $(\mathbf{C}, \mathbf{C}^*, \mathbf{D}, \mathbf{D}^*, \boldsymbol{\Omega}_m)|\boldsymbol{\theta}_{\backslash(\mathbf{C}, \mathbf{C}^*, \mathbf{D}, \mathbf{D}^*, \boldsymbol{\Omega}_m)}, \boldsymbol{m}, \boldsymbol{h}, \boldsymbol{h}^*, \boldsymbol{z}$
10. Go to Step 2

where $\boldsymbol{\theta}_{\backslash\boldsymbol{\delta}}$ denote the parameter $\boldsymbol{\theta}$ excluding $\boldsymbol{\delta}$.

Generation of $\mathbf{h}$

Lopes et al. (2014) implemented the mixture sampler (Kim et al., 1998; Omori et al., 2007) for diagonal components of the decomposed covariance matrix, which transforms the nonlinear measurement equation of individual SV models into a linear equation by using the logarithm of squared daily returns and approximates the distribution of the non-normal disturbances ($\log\chi_1^2$ distribution) by the mixture of normals. Given the component of the mixture of normals, the model reduces to the linear and Gaussian state space model, and hence, we can sample $\{h_{ii,t}\}_{t=1}^{n}$ for $i = 1, \ldots, p$ simutaneously using a simulation smoother (Durbin and Koopman, 2002; de Jong and Shephard, 1995). The mixture sampler approach is a highly efficient estimation strategy, but it needs to correct the approximation error by an additional reweighting step. Alternatively, the multi-move sampler that samples a block of $\{h_{ijt}\}_{t=s}^{t=s+m}$ given other h_{ijs}'s is also known to be efficient to sample these latent volatility variables in the univariate SV models (Omori and Watanabe, 2008; Shephard and Pitt, 1997; Watanabe and Omori, 2004). However, such estimation approaches based on the univariate SV model cannot be applied to our model unless $\mathbf{R}$ is diagonal and $\mathbf{S} = \mathbf{I}_p$. Thus, in this paper, we use the single-move sampler that samples $\boldsymbol{h}_t$ given other $\boldsymbol{h}_s$'s instead and improves the estimation efficiency by incorporating additional measurement equations of the logarithm of the realized variances, $\boldsymbol{x}_t$, without approximating the error distribution by the mixture of normals. We shall show that this is a simple but efficient estimation strategy.

We conduct an MH algorithm using a single-move sampler to generate $\boldsymbol{h}_t$ given other parameters and latent variables. Let $I(A)$ denote an indicator function such that $I(A) = 1$ when A is true and 0 otherwise. The log conditional posterior density is

$$\log \pi (\boldsymbol{h}_t | \boldsymbol{\theta}, \boldsymbol{h}_{-t}, \boldsymbol{h}^*, \boldsymbol{m}, \boldsymbol{z}) = \text{const.} + g(\boldsymbol{h}_t) - \frac{1}{2}(\boldsymbol{h}_t - \boldsymbol{f}_t)' \mathbf{F}_t^{-1}(\boldsymbol{h}_t - \boldsymbol{f}_t),$$

where

$$g(\boldsymbol{h}_t) = -\frac{1}{2}(\boldsymbol{y}_t - \boldsymbol{m}_t)' \mathbf{H}_t^{*\prime} \mathbf{V}_t^{-1/2}(\mathbf{I} + \mathbf{R}'\mathbf{S}'\mathbf{D}^{-1}\mathbf{S}\mathbf{R})\mathbf{V}_t^{-1/2}\mathbf{H}_t^*(\boldsymbol{y}_t - \boldsymbol{m}_t)$$
$$+ (\boldsymbol{y}_t - \boldsymbol{m}_t)' \mathbf{H}_t^{*\prime} \mathbf{V}_t^{-1/2}\mathbf{R}'\mathbf{S}'\mathbf{D}^{-1}\mathbf{S}\{\boldsymbol{h}_{t+1} - \boldsymbol{\mu} - \boldsymbol{\Phi}(\boldsymbol{h}_t - \boldsymbol{\mu})\}I(t < n),$$
$$\mathbf{F}_t^{-1} = \boldsymbol{\Phi}\mathbf{S}'\mathbf{D}^{-1}\mathbf{S}\boldsymbol{\Phi}I(t < n) + \lambda^{-I(t=1)}\mathbf{S}'\mathbf{D}^{-1}\mathbf{S} + \mathbf{C}^{-1},$$
$$\boldsymbol{f}_t = \mathbf{F}_t\Big[-\frac{1}{2}\mathbf{1}_p + \boldsymbol{\Phi}\mathbf{S}'\mathbf{D}^{-1}\mathbf{S}\{\boldsymbol{h}_{t+1} - (\mathbf{I}_p - \boldsymbol{\Phi})\boldsymbol{\mu}\}I(t < n) + \mathbf{C}^{-1}(\boldsymbol{x}_t - \xi\mathbf{1}_p)$$
$$+ \lambda^{-I(t=1)}\mathbf{S}'\mathbf{D}^{-1}\mathbf{S}\big\{(\mathbf{I}_p - \boldsymbol{\Phi})\boldsymbol{\mu} + \boldsymbol{\Phi}\boldsymbol{h}_{t-1} + \mathbf{R}\mathbf{V}_{t-1}^{-1/2}\mathbf{H}_{t-1}^*(\boldsymbol{y}_{t-1} - \boldsymbol{m}_{t-1})\big\}\Big],$$

with $\boldsymbol{y}_0 \equiv \boldsymbol{m}_0$ and $\boldsymbol{h}_0 \equiv \boldsymbol{\mu}$. We generate a candidate $\boldsymbol{h}_t^\dagger \sim \mathcal{N}(\boldsymbol{f}_t, \mathbf{F}_t)$ and accept it with probability $\min\{1, \exp(g(\boldsymbol{h}_t^\dagger) - g(\boldsymbol{h}_t))\}$.

Generation of $\mathbf{h}^*$

Similar to the generation of $\boldsymbol{h}$, we consider the simple single-move sampling. The key idea here is to consider the representation $\mathbf{H}_t^*(\boldsymbol{y}_t - \boldsymbol{m}_t) \equiv (\boldsymbol{y}_t - \boldsymbol{m}_t) + \mathbf{A}_t \boldsymbol{h}_t^*$ where $\mathbf{A}_t$ is the $p \times k$ matrix composed of the linear functions of $\boldsymbol{y}_t - \boldsymbol{m}_t$. It can then be shown that the conditional posterior distribution is multivariate normal by a simple calculation, and we can easily generate

$$\boldsymbol{h}_t^* \sim \mathcal{N}(\boldsymbol{f}_t^*, \mathbf{F}_t^*),$$

where

$$\mathbf{F}_t^{*-1} = \mathbf{A}_t'\mathbf{V}_t^{-1}\mathbf{A}_t + \lambda^{*-I(t=1)}\mathbf{D}^{*-1} + \mathbf{C}^{*-1} + \{\mathbf{A}_t'\mathbf{V}_t^{-1/2}\mathbf{R}'\mathbf{S}'\mathbf{D}^{-1}\mathbf{S}\mathbf{R}\mathbf{V}_t^{-1/2}\mathbf{A}_t + \boldsymbol{\Phi}^*\mathbf{D}^{*-1}\boldsymbol{\Phi}^*\}I(t < n),$$

and

$$\boldsymbol{f}_t^* = \mathbf{F}_t^*\Big[-\mathbf{A}_t'\mathbf{V}_t^{-1}\boldsymbol{y}_t + \mathbf{C}^{*-1}(\boldsymbol{x}_t^* - \boldsymbol{\xi}^*) + \lambda^{*-I(t=1)}\mathbf{D}^{*-1}\big\{(\mathbf{I}_K - \boldsymbol{\Phi}^*)\boldsymbol{\mu}^* + \boldsymbol{\Phi}^*\boldsymbol{h}_{t-1}^*\big\}$$
$$+ \mathbf{A}_t'\mathbf{V}_t^{-1/2}\mathbf{R}'\mathbf{S}'\mathbf{D}^{-1}\mathbf{S}\big\{\boldsymbol{h}_{t+1} - \boldsymbol{\mu} - \boldsymbol{\Phi}(\boldsymbol{h}_t - \boldsymbol{\mu}) - \mathbf{R}\mathbf{V}_t^{-1/2}(\boldsymbol{y}_t - \boldsymbol{m}_t)\big\}I(t < n)$$
$$+ \boldsymbol{\Phi}^*\mathbf{D}^{*-1}\big\{\boldsymbol{h}_{t+1}^* - (\mathbf{I}_K - \boldsymbol{\Phi}^*)\boldsymbol{\mu}^*\big\}I(t < n)\Big],$$

with $\boldsymbol{h}_0^* \equiv \boldsymbol{\mu}^*$ and $K = p(p - 1)/2$. Although the above algorithm is simple and efficient, we note that we could instead use a simulation smoother to generate $\{h_{ijt}\}_{t=1}^n$ for $i > j$ given $\{h_{ikt}\}_{t=1}^n$ ($k \neq j$) as in Lopes et al. (2014) when $\mathbf{R}$ is diagonal and $\mathbf{S} = \mathbf{I}_p$.

Generation of $\mathbf{m}$

Noting that $\boldsymbol{\epsilon}_t | \boldsymbol{\eta}_t \sim \mathcal{N}(\mathbf{R}'(\mathbf{RR}' + \mathbf{S}^{-1}\mathbf{D}\mathbf{S}^{-1\prime})^{-1}\boldsymbol{\eta}_t, \mathbf{I}_p - \mathbf{R}'(\mathbf{RR}' + \mathbf{S}^{-1}\mathbf{D}\mathbf{S}^{-1\prime})^{-1}\mathbf{R})$, we define

$$\tilde{\boldsymbol{y}}_t = \boldsymbol{y}_t - \mathbf{H}_t^{*-1}\mathbf{V}_t^{1/2}\mathbf{R}'(\mathbf{RR}' + \mathbf{S}^{-1}\mathbf{D}\mathbf{S}^{-1\prime})^{-1}\{\boldsymbol{h}_{t+1} - \boldsymbol{\mu} - \boldsymbol{\Phi}(\boldsymbol{h}_t - \boldsymbol{\mu})\}I(t < n),$$
$$\boldsymbol{\Gamma}_t = \mathbf{H}_t^{*-1}\mathbf{V}_t^{1/2}\big\{\mathbf{I}_p - \mathbf{R}'(\mathbf{RR}' + \mathbf{S}^{-1}\mathbf{D}\mathbf{S}^{-1\prime})^{-1}\mathbf{R}I(t < n)\big\}\mathbf{V}_t^{1/2}\mathbf{H}_t^{*-1\prime}.$$

The conditional posterior distribution of $\boldsymbol{m}$ is then the same as that of the following linear Gaussian state space model

$$\tilde{\boldsymbol{y}}_t = \boldsymbol{m}_t + \tilde{\boldsymbol{\epsilon}}_t, \quad \tilde{\boldsymbol{\epsilon}}_t \sim \mathcal{N}(\mathbf{0}, \boldsymbol{\Gamma}_t),$$
$$\boldsymbol{m}_{t+1} = \boldsymbol{m}_t + \boldsymbol{v}_t, \quad \boldsymbol{v}_t \sim \mathcal{N}(\mathbf{0}, \boldsymbol{\Omega}_m),$$

where $\tilde{\boldsymbol{\epsilon}}_t$ and $\boldsymbol{v}_t$ are independent. Thus, we use a simulation smoother for the linear and Gaussian state space model to generate $\{\boldsymbol{m}_t\}_{t=1}^n$ simultaneously (see e.g. Durbin and Koopman, 2002; de Jong and Shephard, 1995).

Generation of R

Let $\boldsymbol{r} = \text{vec}(\mathbf{R}) = (\boldsymbol{r}_1', \ldots, \boldsymbol{r}_p')'$ where $\boldsymbol{r}_j$ denotes the jth column of $\mathbf{R}$. For the prior distribution of $\boldsymbol{r}$, we assume

$$\boldsymbol{r} \sim \mathcal{N}(\boldsymbol{\gamma}_0, \boldsymbol{\Gamma}_0).$$

Noting that $\text{vec}(\mathbf{AB}) = (\mathbf{B}' \otimes \mathbf{I}_n)\text{vec}(\mathbf{A})$ for an $n \times m$ matrix $\mathbf{A}$ and an $m \times q$ matrix $\mathbf{B}$, we have

$$\text{vec}\big\{\mathbf{R}\mathbf{V}_t^{-1/2}\mathbf{H}_t^*(\boldsymbol{y}_t - \boldsymbol{m}_t)\big\} = \big\{(\boldsymbol{y}_t - \boldsymbol{m}_t)'\mathbf{H}_t^{*\prime}\mathbf{V}_t^{-1/2} \otimes \mathbf{I}_p\big\}\boldsymbol{r}.$$

Then, it can be shown that the conditional posterior distribution of r is

$$r|\theta_{\backslash \mathbf{R}}, m, h, h^*, z \sim \mathcal{N}(\gamma_1, \Gamma_1),$$

where

$$\Gamma_1^{-1} = \Gamma_0^{-1} + \left\{ \sum_{t=1}^{n-1} \mathbf{V}_t^{-1/2} \mathbf{H}_t^* (y_t - m_t)(y_t - m_t)' \mathbf{H}_t^{*\prime} \mathbf{V}_t^{-1/2} \right\} \otimes (\mathbf{S}' \mathbf{D}^{-1} \mathbf{S}),$$

$$\gamma_1 = \Gamma_1 \left[\Gamma_0^{-1} \gamma_0 + \left\{ \mathbf{Q} \otimes (\mathbf{S}' \mathbf{D}^{-1} \mathbf{S}) \right\} \mathrm{vec}(\mathbf{I}_p) \right],$$

$$\mathbf{Q} = \sum_{t=1}^{n-1} \mathbf{V}_t^{-1/2} \mathbf{H}_t^* (y_t - m_t)(h_{t+1} - \mu - \Phi(h_t - \mu))'.$$

Alternative parsimonious specification for **R**. In the empirical studies of the factor-based models, it is often that only the first factor (which corresponds to the market factor) shows the leverage effects. Considering such empirical results that we shall also see in our empirical studies, it is useful to study the parsimonious parameterization $\mathbf{R} = \{r_1, 0, \dots, 0\}$. It implies that only the first component of the standardized vector $\mathbf{V}_t^{-1/2} \mathbf{H}_t^* (y_t - m_t)$, which is expected to include the market factor, produces the leverage effect. Thus, we assume

$$\mathbf{R} = \{r_1, 0, \dots, 0\}, \quad r_1 \sim \mathcal{N}(\gamma_{10}, \Gamma_{10}),$$

and then $\mathrm{vec}(\mathbf{R}) = (r_1', 0', \dots, 0')' = e_1 \otimes r_1$ where $e_1 = (1, 0, \dots, 0)'$ is a $p \times 1$ vector. Noting that

$$\mathrm{vec}\left\{ \mathbf{R} \mathbf{V}_t^{-1/2} \mathbf{H}_t^* (y_t - m_t) \right\} = \left\{ (y_t - m_t)' \mathbf{H}_t^{*\prime} \mathbf{V}_t^{-1/2} \otimes \mathbf{I}_p \right\} \{ e_1 \otimes r_1 \}$$

$$= \{ (y_t - m_t)' \mathbf{H}_t^{*\prime} \mathbf{V}_t^{-1/2} e_1 \} r_1,$$

we obtain the conditional posterior distribution of r_1:

$$r_1 | \theta_{\backslash \mathbf{R}}, m, h, h^*, z \sim \mathcal{N}(\gamma_{11}, \Gamma_{11}),$$

where

$$\Gamma_{11}^{-1} = \Gamma_{10}^{-1} + \left[\sum_{t=1}^{n-1} \{ e_1' \mathbf{V}_t^{-1/2} \mathbf{H}_t^* (y_t - m_t) \}^2 \right] \mathbf{S}' \mathbf{D}^{-1} \mathbf{S},$$

$$\gamma_{11} = \Gamma_{11} \left[\Gamma_{10}^{-1} \gamma_{10} + \mathbf{S}' \mathbf{D}^{-1} \mathbf{S} \sum_{t=1}^{n-1} \{ e_1' \mathbf{V}_t^{-1/2} \mathbf{H}_t^* (y_t - m_t) \} (h_{t+1} - \mu - \Phi(h_t - \mu)) \right].$$

Generation of S

Let $s = (s_{21}, \dots, s_{p1}, s_{32}, \dots, s_{p\,p-1})'$ denote a stacked vector of lower off-diagonal elements of $\mathbf{S}$. For the prior distribution of s, we assume

$$s \sim \mathcal{N}(\delta_0, \Delta_0).$$

Using the same idea as that in the generation of h^*, we consider the representation of $\mathbf{S}\tilde{h}_{t+1} = \tilde{h}_{t+1} + \mathbf{B}_{t+1} s$ where $\tilde{h}_{t+1} = h_{t+1} - \mu - \Phi(h_t - \mu) - \mathbf{R}\mathbf{V}_t^{-1/2} \mathbf{H}_t^* (y_t - m_t)$, we obtain the conditional posterior distribution of s:

$$s | \theta_{\backslash \mathbf{S}}, m, h, h^*, z \sim \mathcal{N}(\delta_1, \Delta_1),$$

where

$$\Delta_1^{-1} = \Delta_0^{-1} + \sum_{t=1}^{n} \lambda^{-I(t=1)} \mathbf{B}_t' \mathbf{D}^{-1} \mathbf{B}_t, \quad \delta_1 = \Delta_1 \left[\Delta_0^{-1} \delta_0 - \sum_{t=1}^{n} \lambda^{-I(t=1)} \mathbf{B}_t' \mathbf{D}^{-1} \tilde{h}_t \right].$$

Other details of the MCMC algorithm are rather straightforward and described in Appendix A.

4. Simulation exercise

Simulation set up. To illustrate the MCMC estimation for our proposed model, we generate $n = 2000$ observations where the dimension of asset returns is $p = 9$, which is the same dimension as that used in empirical studies. We set the true values of parameters as $\mu_{ii} = \mu_{ij} = 0$, $\xi = \xi_{ij} = -0.5$, $\phi_{ii} = 0.97$, $\phi_{ij} = 0.99$, $s_{ij} = 0.2$, $\tau_{ii} = 0.1$, $\tau_{ij} = 0.01$, $\sigma_{u,ii} = 0.1$, $\sigma_{u,ij} = 0.1$, $\sigma_{mi} = 0.002$, for $i = 1, \dots, p$, and $j = 1, \dots, i - 1$, and $\mathbf{R} = \{-0.05 \times \mathbf{1}_p, \mathbf{O}\}$.

Table 1

Estimation results for $(\mu, \phi, \xi, \mathbf{C}, \mathbf{D}, \Omega_m)$ for simulated data: bold font means that 95% credible interval does not include true value.

Parameter	True	Mean	95% interval	IF	Parameter	True	Mean	95% interval	IF
μ_{11}	0	0.047	[−0.099, 0.207]	11.0	ϕ_{11}	0.97	0.971	[0.963, 0.979]	5.9
μ_{22}	0	0.148	[−0.002, 0.313]	8.4	ϕ_{22}	0.97	0.970	[0.962, 0.978]	4.7
μ_{33}	0	0.104	[−0.028, 0.247]	13.1	ϕ_{33}	0.97	0.967	[0.959, 0.974]	6.0
μ_{44}	0	0.043	[−0.102, 0.201]	11.3	ϕ_{44}	0.97	0.968	[0.960, 0.975]	4.2
μ_{55}	0	0.169	**[0.048, 0.296]**	13.0	ϕ_{55}	0.97	0.959	**[0.951, 0.967]**	3.7
μ_{66}	0	0.128	[−0.041, 0.306]	7.8	ϕ_{66}	0.97	0.969	[0.962, 0.977]	5.4
μ_{77}	0	0.065	[−0.104, 0.243]	7.5	ϕ_{77}	0.97	0.969	[0.962, 0.976]	5.1
μ_{88}	0	0.155	[−0.044, 0.364]	6.5	ϕ_{88}	0.97	0.970	[0.963, 0.977]	5.3
μ_{99}	0	0.142	[−0.059, 0.346]	5.7	ϕ_{99}	0.97	0.968	[0.961, 0.974]	2.9
τ_{11}	0.1	0.098	[0.093, 0.104]	26.8	ξ	−0.5	−0.496	[−0.518, −0.478]	569.0
τ_{22}	0.1	0.100	[0.095, 0.106]	21.2					
τ_{33}	0.1	0.094	[0.089, 0.100]	25.5					
τ_{44}	0.1	0.098	[0.093, 0.105]	21.4					
τ_{55}	0.1	0.101	[0.095, 0.107]	17.8					
τ_{66}	0.1	0.104	[0.098, 0.110]	26.9					
τ_{77}	0.1	0.096	[0.090, 0.103]	33.0					
τ_{88}	0.1	0.104	[0.098, 0.110]	22.3					
τ_{99}	0.1	0.107	**[0.101, 0.113]**	22.6					
$\sigma_{u, 11}$	0.1	0.103	[0.098, 0.108]	18.7	σ_{m1}	0.002	0.0021	[0.0009, 0.0043]	561.8
$\sigma_{u, 22}$	0.1	0.099	[0.095, 0.104]	17.1	σ_{m2}	0.002	0.0020	[0.0008, 0.0047]	592.5
$\sigma_{u, 33}$	0.1	0.101	[0.096, 0.106]	22.9	σ_{m3}	0.002	0.0016	[0.0006, 0.0050]	654.3
$\sigma_{u, 44}$	0.1	0.104	[0.098, 0.108]	22.7	σ_{m4}	0.002	0.0022	[0.0009, 0.0045]	569.5
$\sigma_{u, 55}$	0.1	0.0977	[0.093, 0.102]	17.4	σ_{m5}	0.002	0.0010	[0.0003, 0.0025]	642.1
$\sigma_{u, 66}$	0.1	0.0978	[0.092, 0.103]	18.7	σ_{m6}	0.002	0.0029	[0.0014, 0.0053]	528.9
$\sigma_{u, 77}$	0.1	0.100	[0.095, 0.106]	32.1	σ_{m7}	0.002	0.0022	[0.0011, 0.0041]	533.3
$\sigma_{u, 88}$	0.1	0.094	[0.088, 0.100]	25.0	σ_{m8}	0.002	0.0015	[0.0006, 0.0037]	620.4
$\sigma_{u, 99}$	0.1	0.094	[0.088, 0.104]	20.1	σ_{m9}	0.002	0.0010	[0.0004, 0.0028]	636.2

Table 2

Posterior means of $\mathbf{R}$ for simulated data: bold font means that 95% credible interval does not include true value.

r_{ij}	$j = 1$	$j = 2$	$j = 3$	$j = 4$	$j = 5$	$j = 6$	$j = 7$	$j = 8$	$j = 9$
$i = 1$	−0.0480	−0.0008	−0.0025	0.0011	0.0010	−0.0042	−0.0042	0.0015	−0.0015
$i = 2$	−0.0522	0.0016	0.0009	0.0009	−0.0039	0.0023	−0.0044	−0.0004	0.0010
$i = 3$	−0.0524	−0.0020	−0.0017	0.0029	−0.0003	0.0014	0.0010	−0.0024	−0.0012
$i = 4$	−0.0510	−0.0054	−0.0002	0.0054	−0.0008	0.0007	−0.0030	−0.0053	−0.0008
$i = 5$	−0.0532	−0.0041	−0.0030	0.0005	0.0021	−0.0014	−0.0003	0.0035	**0.0065**
$i = 6$	−0.0485	−0.0019	−0.0059	0.0013	0.0010	−0.0002	**−0.0098**	0.0000	0.0020
$i = 7$	−0.0497	−0.0040	−0.0049	−0.0020	0.0034	−0.0053	−0.0045	0.0039	−0.0028
$i = 8$	−0.0520	0.0021	−0.0036	−0.0012	0.0039	−0.0017	−0.0039	−0.0026	−0.0049
$i = 9$	−0.0464	−0.0036	0.0002	0.0003	0.0046	0.0040	−0.0020	0.0006	−0.0005

Prior set up. The prior distributions of parameters are assumed to be

$$\mu_{ii} \sim \mathcal{N}(0, 10^2), \quad \mu_{ij} \sim \mathcal{N}(0, 10^2), \quad \xi \sim \mathcal{N}(0, 10^2), \quad \xi_{ij} \sim \mathcal{N}(0, 10^2),$$

$$\phi_{ii} \sim \mathcal{U}(-1, 1), \quad \phi_{ij} \sim \mathcal{U}(-\sqrt{1.3}, \sqrt{1.3}), \quad s_{ij} \sim \mathcal{N}(0, 10^2),$$

$$\tau_{ii}^2 \sim \mathcal{IG}(5, 0.05), \quad \sigma_{u,ii}^2 \sim \mathcal{IG}(5, 0.05), \quad \sigma_{u,ij}^2 \sim \mathcal{IG}(5, 0.05),$$

$$\tau_{ij}^2 \sim \mathcal{IG}(10^{-4}, 10^{-4}), \quad \sigma_{mi}^2 \sim \mathcal{IG}(10^{-6}, 10^{-6}),$$

for $i = 1, \ldots, p$, and $j = 1, \ldots, i-1$, and $r_{ij} \sim \mathcal{N}(0, 10^2)$ for $i, j = 1, \ldots, p$. We assume fairly flat prior distributions for μ, μ^*, ξ, ξ^*, r, s and flat prior distributions for ϕ, ϕ^*. For error variances of the diagonal components (τ_{ii}^2) and realized measures ($\sigma_{u,ii}^2, \sigma_{u,ij}^2$), we assume inverse gamma prior distributions $\mathcal{IG}(5, 0.05)$ which are often used in the literature. For error variances of nondiagonal components (τ_{ij}^2) and the mean return process m_t, we put $\mathcal{IG}(\epsilon, \epsilon)$ prior distributions with small ϵ as discussed in the previous section. For the hyperparameters, $(\lambda, \lambda^*, \lambda_m)$, we set $\lambda = \lambda^* = \lambda_m = 100$ to remove the influence of initial values.

MCMC set up. The number of iterations for MCMC is 90,000. The first 60,000 samples are discarded as the burn-in period. Tables 1–3 show the estimation results for $(\mu, \phi, \xi, \mathbf{C}, \mathbf{D}, \Omega_m)$, $\mathbf{R}$ and $\mathbf{S}$ for the diagonal components h, while Tables 4–8 show the estimation results for $(\mu^*, \phi^*, \xi^*, \mathbf{C}^*, \mathbf{D}^*)$ for the nondiagonal components h^*. The posterior means of parameters are close to their true values and 95% credible intervals include these true values in most cases.

Table 3
Posterior means of S for simulated data: bold font means that 95% credible interval does not include true value.

s_{ij}	$j = 1$	$j = 2$	$j = 3$	$j = 4$	$j = 5$	$j = 6$	$j = 7$	$j = 8$	$j = 9$
$i = 1$	1								
$i = 2$	0.212	1							
$i = 3$	0.266	**0.126**	1						
$i = 4$	0.245	0.189	0.178	1					
$i = 5$	0.179	0.193	0.194	0.244	1				
$i = 6$	0.180	0.218	0.214	0.193	0.204	1			
$i = 7$	0.163	0.253	0.274	0.223	0.213	0.100	1		
$i = 8$	0.180	0.236	0.255	0.218	0.179	0.204	0.173	1	
$i = 9$	0.277	0.183	0.165	0.189	0.183	0.266	0.224	0.133	1

Table 4
Posterior means of μ^* for simulated data: bold font means that 95% credible interval does not include true value.

μ_{ij}	$j = 1$	$j = 2$	$j = 3$	$j = 4$	$j = 5$	$j = 6$	$j = 7$	$j = 8$
$i = 2$	0.024							
$i = 3$	−0.009	0.010						
$i = 4$	−0.032	0.003	−0.007					
$i = 5$	−0.001	−0.033	0.008	−0.006				
$i = 6$	0.012	−0.045	0.028	0.034	−0.013			
$i = 7$	−0.050	0.017	−0.016	0.023	−0.014	−0.017		
$i = 8$	−0.016	**−0.059**	0.031	0.028	−0.008	−0.013	−0.001	
$i = 9$	−0.003	0.005	**−0.057**	−0.012	0.011	0.035	−0.025	−0.012

Table 5
Posterior means of ϕ^* for simulated data: bold font means that 95% credible interval does not include true value.

ϕ_{ij}	$j = 1$	$j = 2$	$j = 3$	$j = 4$	$j = 5$	$j = 6$	$j = 7$	$j = 8$
$i = 2$	0.993							
$i = 3$	0.987	0.991						
$i = 4$	0.987	0.986	0.990					
$i = 5$	0.990	0.989	0.986	0.994				
$i = 6$	0.986	0.988	0.989	0.991	0.989			
$i = 7$	**0.975**	0.989	0.986	0.989	**0.980**	0.988		
$i = 8$	0.990	0.989	0.987	0.994	0.989	0.988	0.982	
$i = 9$	0.987	0.985	0.989	0.989	0.992	**0.980**	0.993	0.989

Table 6
Posterior means of ξ^* for simulated data: bold font means that 95% credible interval does not include true value.

ξ_{ij}	$j = 1$	$j = 2$	$j = 3$	$j = 4$	$j = 5$	$j = 6$	$j = 7$	$j = 8$
$i = 2$	−0.4916							
$i = 3$	−0.5022	−0.5005						
$i = 4$	−0.4920	−0.4966	−0.4979					
$i = 5$	−0.5137	−0.4788	−0.4961	−0.4917				
$i = 6$	−0.5032	−0.4815	−0.5288	−0.5299	−0.5356			
$i = 7$	−0.4754	−0.5009	−0.4889	−0.5212	−0.5070	−0.5098		
$i = 8$	−0.5059	**−0.4681**	−0.5165	−0.5216	−0.5122	−0.5069	−0.4843	
$i = 9$	−0.5021	−0.4793	**−0.4557**	−0.4775	−0.4989	−0.5061	−0.4843	**−0.4721**

Table 7
Posterior means of C^* for simulated data: bold font means that 95% credible interval does not include true value.

μ_{ij}	$j = 1$	$j = 2$	$j = 3$	$j = 4$	$j = 5$	$j = 6$	$j = 7$	$j = 8$
$i = 2$	0.099							
$i = 3$	0.099	**0.103**						
$i = 4$	0.101	0.099	0.099					
$i = 5$	0.101	0.100	0.101	0.099				
$i = 6$	0.101	0.099	0.100	**0.097**	**0.103**			
$i = 7$	0.098	0.098	0.100	0.098	0.101	0.099		
$i = 8$	0.098	0.098	0.099	0.099	0.100	0.101	0.101	
$i = 9$	0.100	0.099	0.099	0.098	0.100	0.100	0.100	**0.0972**

Table 8
Posterior means of $\boldsymbol{D}^*$ for simulated data: bold font means that 95% credible interval does not include true value.

τ_{ij}	$j=1$	$j=2$	$j=3$	$j=4$	$j=5$	$j=6$	$j=7$	$j=8$
$i=2$	0.0098							
$i=3$	0.0096	0.0098						
$i=4$	0.0101	**0.0120**	0.0097					
$i=5$	0.0106	0.0112	0.0099	**0.0078**				
$i=6$	0.0088	0.0105	0.0115	0.0105	0.0093			
$i=7$	0.0119	0.0103	0.0105	0.0102	0.0117	0.0105		
$i=8$	0.0098	0.0087	0.0106	0.0089	0.0097	0.0107	0.0110	
$i=9$	0.0104	0.0102	0.0103	0.0108	0.0099	0.0119	0.0098	0.0106
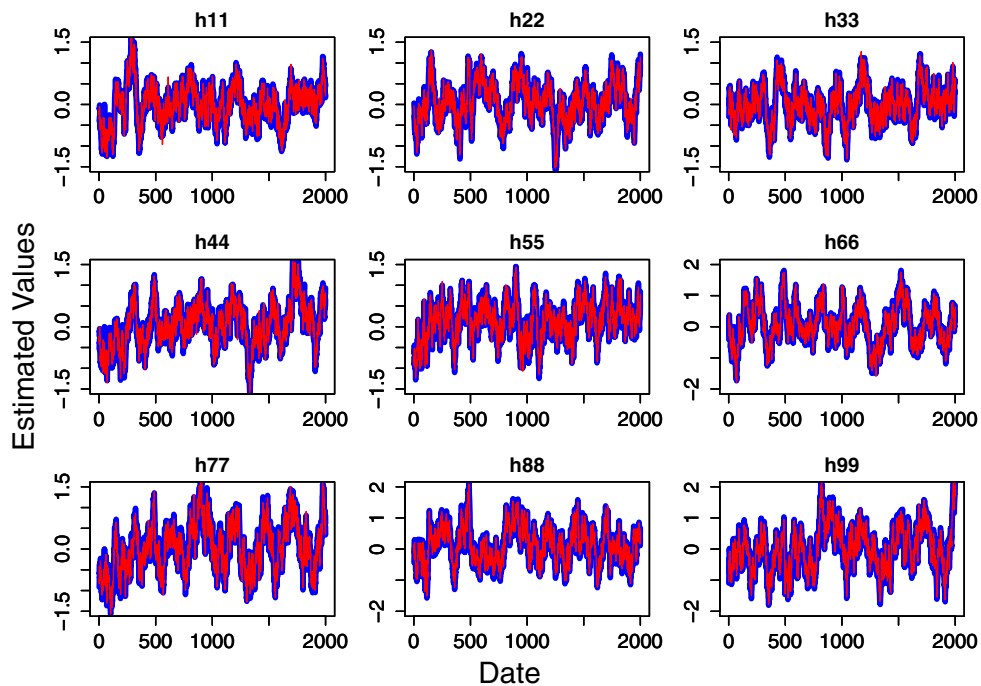
Fig. 1. 95% credible intervals (blue) and true values (red) for $h_{11,t}, \ldots, h_{99,t}$. (For interpretation of the references to color in this figure legend, the reader is referred to the web version of this article.)

Fig. 1 shows estimated 95% credible intervals for $\boldsymbol{h}_t$ with true values. The estimated intervals cover the true values and capture the dynamic behavior of these diagonal components. Further, estimated dynamic correlations between asset returns for $(\rho_{21,t}, \ldots, \rho_{62,t})$ are shown in Fig. 2. These true values are also included in 95% credible intervals and are well estimated.

5. Application to U.S. stock returns

The proposed model is applied to daily returns and realized covariances of nine U.S. stocks ($p=9$): JP Morgan (JPM), International Business Machine (IBM), Microsoft (MSFT), Exxon Mobil (XOM), Alcoa (AA), American Express (AXP), Du Pont (DD), General Electric (GE), and Coca Cola (KO). The realized covariance for these assets can be downloaded from Oxford Man Institute website (see, Heber et al., 2009; Noureldin et al., 2012). Although the dataset also includes Bank of America (BA), because it has an extremely high volatility period after the financial crisis, it is excluded from our empirical studies.

The daily returns for the ith stock are defined as $y_{it} = 100 \times (\log p_{it} - \log p_{i,t-1})$, where p_{it} is the close value of the ith asset at time t. The realized covariance is calculated by 5-min intraday returns with subsampling. The number of observations is $n = 2242$ (February 1, 2001 to December 31, 2009). We note that this dataset includes the high volatility period after the financial crisis in 2008 as shown in Fig. 3.

5.1. Estimation results

Estimation efficiencies for CSV and CRSV models. First, we compare the estimation results of CSV and CRSV models by using the single-move sampler. The number of iterations for MCMC is 90,000. The first 60,000 samples are discarded as the burn-in period. Table 9 shows a part of estimation results for the diagonal components. We see that the estimation of the CRSV
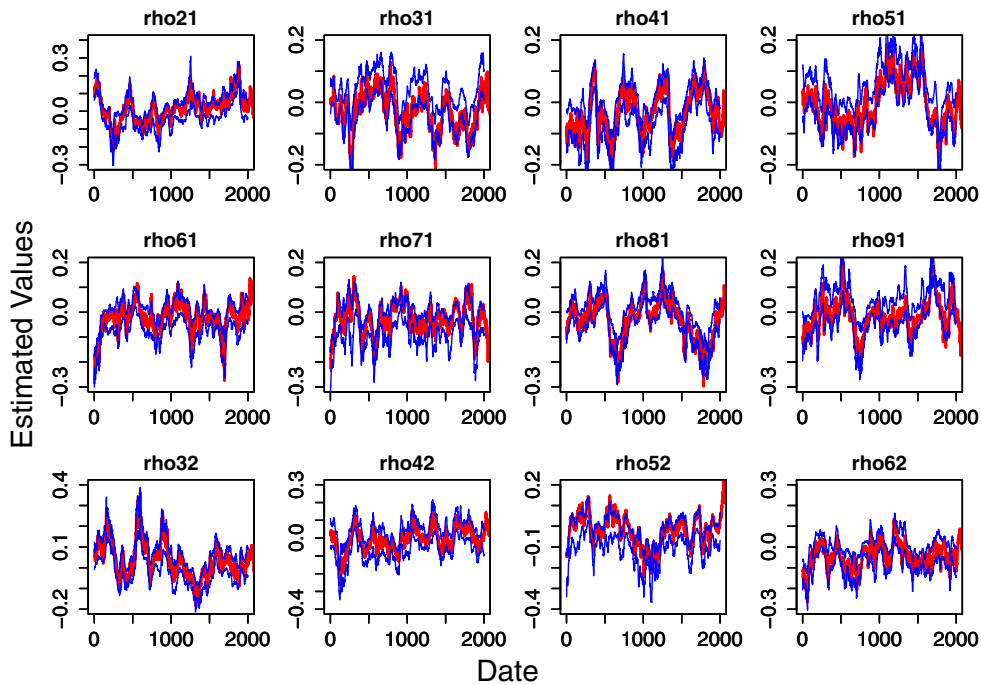
Fig. 2. 95% credible intervals (blue) and true values (red) for dynamic correlations $\rho_{21,t}, \ldots, \rho_{62,t}$. (For interpretation of the references to color in this figure legend, the reader is referred to the web version of this article.)
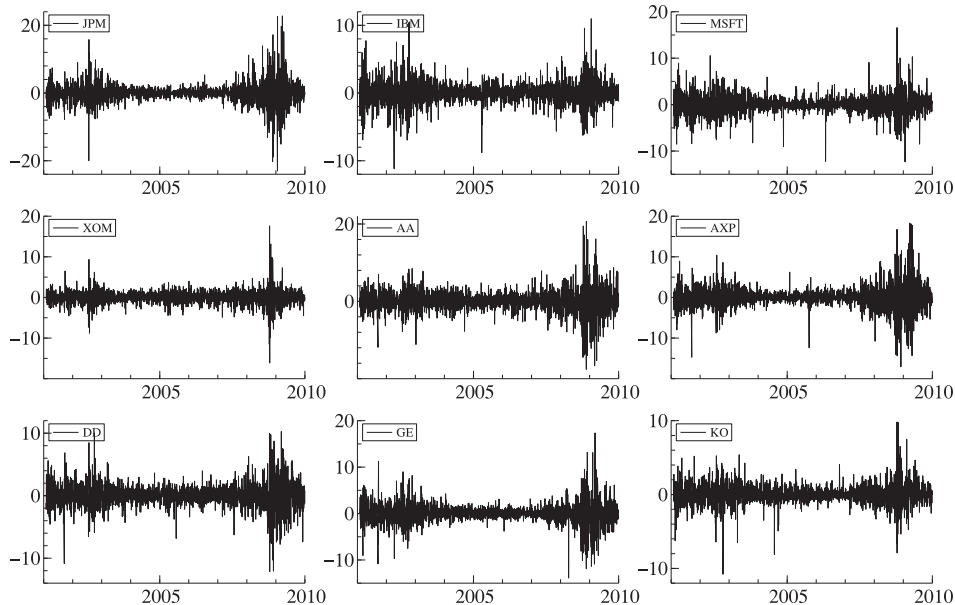
Fig. 3. Time series plot of daily returns, $y_{t1}, \ldots, y_{9t}$.

model is more efficient than that of the CSV model in terms of inefficiency factors (IF). The inefficiency factor is the ratio of the numerical variance of the estimate from the MCMC samples relative to that from hypothetical uncorrelated samples, and is defined as $1 + 2\sum_{s=1}^{\infty} \rho_s$ where ρ_s is the sample autocorrelation at lag s. It suggests the relative number of correlated draws necessary to attain the same variance of the posterior sample mean from the uncorrelated draws (Chib, 2001).

We incorporate diagonal and off-diagonal components of decomposed realized covariance as an additional source of information regarding latent covariance variables. This improves sampling efficiencies and standard deviations of parameters.

Table 9
Estimation results for μ, ϕ, **D** for U.S. stock returns CRSV and CSV models.

CRSV	Mean	Stdev	95% interval	IF	CSV	Mean	Stdev	95% interval	IF
μ_{11}	1.097	0.133	[0.833, 1.360]	3.5	μ_{11}	1.086	0.241	[0.603, 1.560]	21.1
μ_{22}	0.278	0.088	[0.104, 0.452]	4.3	μ_{22}	0.192	0.099	[−0.004, 0.389]	31.8
μ_{33}	0.405	0.091	[0.225, 0.585]	4.1	μ_{33}	0.127	0.106	[−0.085, 0.329]	146.6
μ_{44}	0.290	0.084	[0.126, 0.456]	5.5	μ_{44}	0.259	0.072	[0.117, 0.400]	80.4
μ_{55}	1.095	0.092	[0.913, 1.279]	5.0	μ_{55}	1.023	0.078	[0.870, 1.178]	86.5
μ_{66}	0.435	0.132	[0.178, 0.695]	3.0	μ_{66}	0.225	0.114	[0.002, 0.451]	61.5
μ_{77}	0.296	0.086	[0.126, 0.469]	5.4	μ_{77}	−0.070	0.080	[−0.232, 0.085]	226.7
μ_{88}	0.125	0.106	[−0.083, 0.333]	3.9	μ_{88}	−0.120	0.102	[−0.320, 0.081]	91.5
μ_{99}	−0.169	0.083	[−0.332, −0.004]	5.3	μ_{99}	−0.418	0.095	[−0.608, −0.232]	87.4
ϕ_{11}	0.947	0.004	[0.938, 0.955]	103.1	ϕ_{11}	0.982	0.005	[0.970, 0.991]	431.1
ϕ_{22}	0.930	0.006	[0.917, 0.941]	82.6	ϕ_{22}	0.921	0.014	[0.888, 0.946]	363.3
ϕ_{33}	0.936	0.006	[0.924, 0.947]	78.9	ϕ_{33}	0.867	0.018	[0.830, 0.902]	341.5
ϕ_{44}	0.935	0.006	[0.923, 0.948]	76.5	ϕ_{44}	0.899	0.015	[0.868, 0.926]	367.7
ϕ_{55}	0.944	0.006	[0.933, 0.956]	114.7	ϕ_{55}	0.875	0.020	[0.826, 0.908]	413.5
ϕ_{66}	0.955	0.004	[0.947, 0.963]	122.0	ϕ_{66}	0.931	0.007	[0.914, 0.944]	310.8
ϕ_{77}	0.942	0.005	[0.931, 0.953]	118.2	ϕ_{77}	0.849	0.021	[0.796, 0.882]	394.3
ϕ_{88}	0.941	0.005	[0.931, 0.951]	94.3	ϕ_{88}	0.892	0.011	[0.869, 0.912]	283.7
ϕ_{99}	0.938	0.006	[0.925, 0.950]	72.3	ϕ_{99}	0.848	0.017	[0.811, 0.878]	287.2
τ_{11}	0.328	0.010	[0.308, 0.347]	89.1	τ_{11}	0.179	0.027	[0.134, 0.243]	599.2
τ_{22}	0.140	0.009	[0.122, 0.159]	151.2	τ_{22}	0.333	0.035	[0.269, 0.405]	467.7
τ_{33}	0.129	0.008	[0.113, 0.146]	129.9	τ_{33}	0.535	0.047	[0.440, 0.627]	425.6
τ_{44}	0.141	0.007	[0.127, 0.157]	86.6	τ_{44}	0.251	0.026	[0.204, 0.305]	474.3
τ_{55}	0.113	0.009	[0.096, 0.131]	229.0	τ_{55}	0.345	0.045	[0.269, 0.453]	544.3
τ_{66}	0.109	0.008	[0.093, 0.125]	196.2	τ_{66}	0.251	0.028	[0.194, 0.302]	545.6
τ_{77}	0.087	0.008	[0.072, 0.104]	234.7	τ_{77}	0.316	0.048	[0.247, 0.426]	573.0
τ_{88}	0.127	0.009	[0.108, 0.146]	198.1	τ_{88}	0.308	0.034	[0.253, 0.383]	510.4
τ_{99}	0.128	0.010	[0.109, 0.148]	187.8	τ_{99}	0.419	0.045	[0.343, 0.515]	449.7

Estimation results for diagonal elements $\mathbf{h}_t$. Table 10 shows estimation results (posteior means, posterior standard deviations, 95% credible intervals and inefficiency factors) for μ, ϕ, ξ, **C**, **D** and Ω_m.

Since the posterior means of ϕ_{ii}'s are over 0.9, the persistence of diagonal elements $\mathbf{h}_t$ is high for all i, but they are relatively smaller than those in univariate SV models. This is consistent with previous empirical studies (Takahashi et al., 2009). Estimates of some means of diagonal elements, such as μ_{11} and μ_{55}, are much larger than those of others (especially μ_{88} and μ_{99}), suggesting that there are differences among the magnitude of conditional volatilities. The bias adjustment term ξ is estimated to be −0.366 with 95% credible interval [−0.387, −0.345]. It implies that the scale bias for the realized covariance is close to $\exp(-0.366) \approx 0.693$. This is partly because nontrading hours are not considered in calculating the realized variances. Thus, the construction of covariance estimators solely from the realized covariance would overestimate true volatilities, while one could adjust such a scale bias within CRSV models. Finally, the variances of mean process $\mathbf{m}_t$ are estimated to be small, as we expected, suggesting that there are only small fluctuations in means of $\mathbf{y}_t$.

Fig. 4 shows the estimated posterior 95% credible intervals for $\xi \mathbf{1}_p + \mathbf{h}_t$ with blue lines, where the observed $\mathbf{x}_t (= \xi \mathbf{1}_p + \mathbf{h}_t + \mathbf{u}_t)$ are shown with red lines. The 95% credible intervals are much narrower than the sharp fluctuation of $\mathbf{x}_t$, and were successful in extracting the smooth mean trends of $\xi + h_{ii,t}$ for all i after eliminating the measurement errors.

Table 11 shows the posterior means of elements of **R**, and the red figure indicates that 95% credible interval does not include 0 (in other words, $\Pr(r_{ij} < 0|\text{data}) > 0.975$). The elements of the first column of **R** are found to be much smaller than those of other columns, which implies credible negative effects of $y_{1t} - m_{1t}$ on $\mathbf{h}_{t+1}$. Fig. 5 shows the time series plots of dynamic leverage effects of the first element $\mathbf{H}_t^*(\mathbf{y}_t - \mathbf{m}_t)$ on $\mathbf{h}_{t+1}$, i.e., the first column $\mathbf{l}_{1t} = (L_{11,t}, \ldots, L_{91,t})'$ of $\mathbf{L}_t = \mathbf{R}\mathbf{V}_t^{-1/2}\mathbf{H}_t^*$. The posterior means of all $l_{1j,t}$'s are negative (shown with red lines) and indicate leverage effects on conditional log volatilities. The effect $l_{11,t}$ on the first components $h_{11,t+1}$ is the largest in its absolute value and credible in the sense that 95% credible intervals (shown with blue lines) are below zero. Table 12 shows the posterior means of **S**. There are some positive posterior means with $\Pr(s_{ij} > 0|\text{data}) > 0.975$, and hence, there is a credible positive dependence among $\mathbf{h}_{t+1}$ given $\mathbf{y}_t$.

Estimation results for nondiagonal elements $\mathbf{h}_t^*$. Tables 13 –17 show the estimation results (posteior means, posterior standard deviations) for μ^*, ϕ^*, ξ^*, $\mathbf{C}^*$ and $\mathbf{D}^*$.

The posterior means of μ^* are all positive, which suggests the positive dependence among $\mathbf{y}_t - \mathbf{m}_t$. Considering their standard deviations, all but μ_{9j}'s are credibly positive. The ϕ_{ij}'s are estimated to be close to one as expected, and the error standard deviations τ_{ij}'s are relatively small. The small τ_{ij} indicates that the corresponding $h_{ij,t}$ are close to constant. Fig. 6 shows the estimated posterior 95% credible intervals for off-diagonal components, $\xi_{ij} + h_{ij,t}$ for $i = 2, \ldots, 6$ and $j = 1, 2$ with blue lines, and the red lines show the corresponding off-diagonal components of realized covariance $x_{ij,t} = \xi_{ij} + h_{ij,t} + u_{ij,t}$. While observed $x_{ij,t}$'s seem to have large noises, the 95% credible intervals are much narrower and stable. This is consistent

Table 10

Estimation result for $\boldsymbol{\mu}$, $\boldsymbol{\phi}$, ξ, $\mathbf{C}$, $\mathbf{D}$, $\boldsymbol{\Omega}_m$ for U.S. stock returns. CRSV model.

Parameter	Mean	95% interval	IF	Parameter	Mean	95% interval	IF
μ_{11}	1.097	[0.833, 1.360]	3.5	ϕ_{11}	0.947	[0.938, 0.955]	103.1
μ_{22}	0.278	[0.104, 0.452]	4.3	ϕ_{22}	0.930	[0.917, 0.941]	82.6
μ_{33}	0.405	[0.225, 0.585]	4.1	ϕ_{33}	0.936	[0.924, 0.947]	78.9
μ_{44}	0.290	[0.126, 0.456]	5.5	ϕ_{44}	0.935	[0.923, 0.948]	76.5
μ_{55}	1.095	[0.913, 1.279]	5.0	ϕ_{55}	0.944	[0.933, 0.956]	114.7
μ_{66}	0.435	[0.178, 0.695]	3.0	ϕ_{66}	0.955	[0.947, 0.963]	122.0
μ_{77}	0.296	[0.126, 0.469]	5.4	ϕ_{77}	0.942	[0.931, 0.953]	118.2
μ_{88}	0.125	[−0.083, 0.333]	3.9	ϕ_{88}	0.941	[0.931, 0.951]	94.3
μ_{99}	−0.169	[−0.332, −0.004]	5.3	ϕ_{99}	0.938	[0.925, 0.950]	72.3
τ_{11}	0.328	[0.308, 0.347]	89.1	ξ	−0.366	[−0.387, −0.345]	156.9
τ_{22}	0.140	[0.122, 0.159]	151.2				
τ_{33}	0.129	[0.113, 0.146]	129.9				
τ_{44}	0.141	[0.127, 0.157]	86.6				
τ_{55}	0.113	[0.096, 0.131]	229.0				
τ_{66}	0.109	[0.093, 0.125]	196.2				
τ_{77}	0.087	[0.072, 0.104]	234.7				
τ_{88}	0.127	[0.108, 0.146]	198.1				
τ_{99}	0.128	[0.109, 0.148]	187.8				
$\sigma_{u,11}$	0.326	[0.312, 0.341]	60.9	σ_{m1}	0.0010	[0.0004, 0.0027]	583.0
$\sigma_{u,22}$	0.314	[0.299, 0.328]	63.9	σ_{m2}	0.0017	[0.0005, 0.0036]	561.2
$\sigma_{u,33}$	0.316	[0.302, 0.330]	56.0	σ_{m3}	0.0012	[0.0003, 0.0034]	623.8
$\sigma_{u,44}$	0.310	[0.298, 0.322]	27.6	σ_{m4}	0.0034	[0.0013, 0.0071]	554.2
$\sigma_{u,55}$	0.356	[0.342, 0.370]	57.1	σ_{m5}	0.0015	[0.0005, 0.0039]	654.1
$\sigma_{u,66}$	0.361	[0.347, 0.375]	54.6	σ_{m6}	0.0012	[0.0004, 0.0053]	626.8
$\sigma_{u,77}$	0.341	[0.327, 0.354]	56.8	σ_{m7}	0.0011	[0.0003, 0.0026]	565.4
$\sigma_{u,88}$	0.333	[0.318, 0.348]	61.9	σ_{m8}	0.0009	[0.0004, 0.0020]	528.2
$\sigma_{u,99}$	0.313	[0.299, 0.327]	57.4	σ_{m9}	0.0014	[0.0005, 0.0039]	608.7

Table 11

Posterior means of $\mathbf{R}$ for U.S. stock returns. CRSV model: bold font indicates that 95% credible interval does not include 0.

r_{ij}	$j=1$	$j=2$	$j=3$	$j=4$	$j=5$	$j=6$	$j=7$	$j=8$	$j=9$
$i=1$	**−0.0585**	−0.0119	−0.0113	−0.0177	−0.0042	−0.0152	0.0047	0.0063	−0.0152
$i=2$	**−0.0291**	**−0.0319**	0.0031	−0.0062	−0.0029	**−0.0169**	−0.0010	−0.0052	−0.0086
$i=3$	**−0.0167**	−0.0144	−0.0095	−0.0007	−0.0002	−0.0064	−0.0022	−0.0040	0.0002
$i=4$	**−0.0319**	−0.0049	**−0.0180**	**−0.0206**	−0.0063	−0.0141	−0.0107	−0.0038	−0.0029
$i=5$	**−0.0276**	−0.0049	−0.0086	−0.0110	−0.0063	−0.0019	−0.0026	−0.0015	−0.0025
$i=6$	**−0.0315**	0.0016	−0.0000	**−0.0211**	−0.0005	**−0.0247**	0.0006	−0.0115	0.0028
$i=7$	**−0.0271**	−0.0125	−0.0081	−0.0064	−0.0075	−0.0072	−0.0002	0.0026	−0.0047
$i=8$	**−0.0295**	−0.0004	−0.0035	−0.0110	−0.0020	−0.0038	0.0042	**−0.0306**	−0.0106
$i=9$	**−0.0289**	−0.0004	−0.0044	−0.0139	0.0007	−0.0127	−0.0062	−0.0082	**−0.0219**

Table 12

Posterior means of $\mathbf{S}$ for U.S. stock returns. CRSV model: bold font indicates that 95% credible interval does not include 0.

s_{ij}	$j=1$	$j=2$	$j=3$	$j=4$	$j=5$	$j=6$	$j=7$	$j=8$	$j=9$
$i=1$	1								
$i=2$	**0.761**	1							
$i=3$	**0.227**	**0.591**	1						
$i=4$	**0.273**	**0.206**	**0.227**	1					
$i=5$	**0.407**	−0.023	−0.045	**0.397**	1				
$i=6$	**0.657**	**−0.188**	**0.227**	**0.239**	−0.095	1			
$i=7$	−0.043	−0.091	**0.195**	**0.236**	**0.193**	**0.402**	1		
$i=8$	0.134	0.159	0.055	−0.146	**0.309**	**0.579**	−0.125	1	
$i=9$	−0.072	**0.337**	−0.112	0.015	−0.071	0.148	**0.507**	0.0639	1

with the posterior estimates of $\sigma_{u,ij}$ whose magnitude is much larger than that of the τ_{ij}. We note that for some off-diagonal components such as h_{61}, h_{52} and h_{54}, there are sharp increases in trends after the financial crisis. Also, there seems to be no clear bias direction in $\boldsymbol{x}_t^*$ since some bias terms ξ_{ij} are estimated to be positive while others are negative.

Finally, Fig. 7 shows the posterior means (with red lines) and 95% credible intervals (with blue lines) for time-varying correlation $\rho_{ij,t}$'s ($i=2,\ldots,6$ and $j=1,2$). We observe the co-movement of the correlation processes among stock returns with the upward trend after financial crisis in 2008.
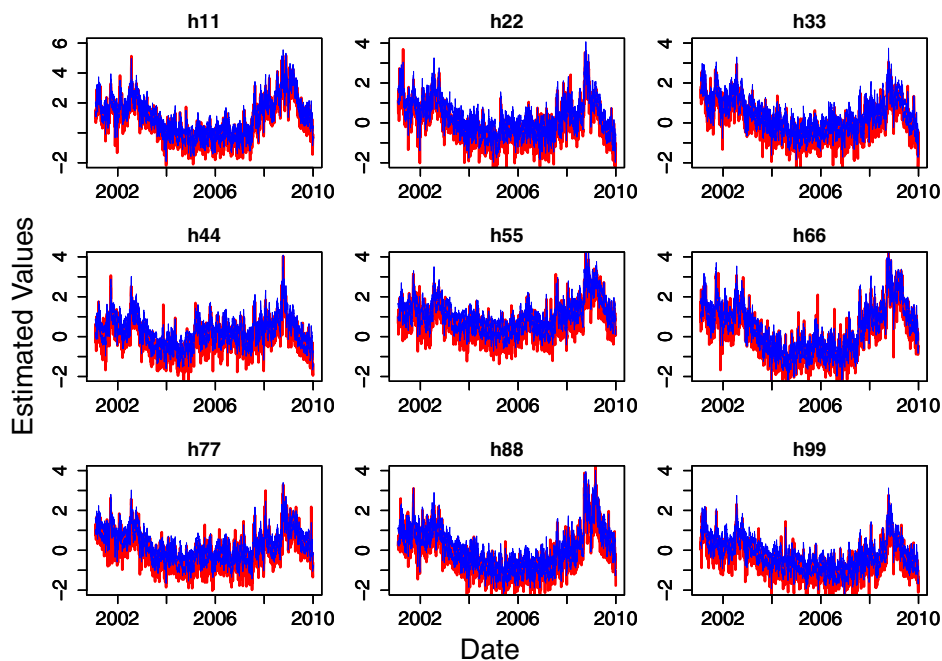
Fig. 4. 95% credible intervals (blue) for $\xi + h_{11,t}, \ldots, \xi + h_{99,t}$, and $x_{1t}, \ldots, x_{9t}$ (red). (For interpretation of the references to color in this figure legend, the reader is referred to the web version of this article.)
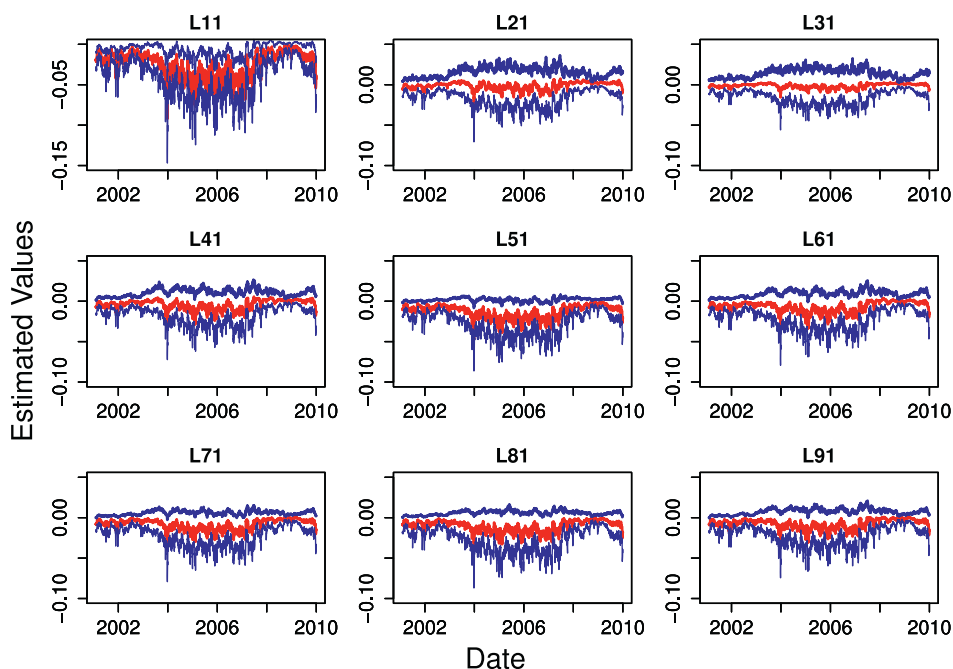
Fig. 5. Posterior means (red) and 95% credible intervals (blue) for $L_{11,t}, \ldots, L_{91,t}$ where $\mathbf{L}_t = \mathbf{RV}_t^{-1/2} \mathbf{H}_t^*$. (For interpretation of the references to color in this figure legend, the reader is referred to the web version of this article.)

5.2. Model comparison based on portfolio performances

For univariate volatility models, it is straightforward to evaluate the forecasting performances: we compare the predictive mean square error (PMSE) using several kinds of loss functions (such as mean square loss, mean absolute loss and quasi likelihood loss. see Patton, 2011). However, for multivariate volatility models, it is difficult to choose appropriate distance measures between two covariance matrices. Furthermore, it is certainly not obvious that all elements of the difference

Table 13

Posterior means (standard deviation) of $\boldsymbol{\mu}^*$ for U.S. stock returns. CRSV model: bold font indicates that 95% credible interval does not include 0.

μ_{ij}	$j = 1$	$j = 2$	$j = 3$	$j = 4$	$j = 5$	$j = 6$	$j = 7$	$j = 8$
$i = 2$	**0.333**							
$i = 3$	**0.210**	**0.484**						
$i = 4$	**0.170**	**0.177**	**0.120**					
$i = 5$	**0.263**	0.168	0.151	0.424				
$i = 6$	**0.419**	0.160	0.105	0.151	0.070			
$i = 7$	**0.139**	0.114	0.085	0.135	0.184	0.113		
$i = 8$	**0.135**	0.145	0.111	0.106	0.057	0.167	0.119	
$i = 9$	**0.058**	0.050	0.060	0.128	0.014	0.055	0.037	0.058

Table 14

Posterior means (standard deviation) of $\boldsymbol{\phi}^*$: U.S. stock returns. CRSV model.

ϕ_{ij}	$j = 1$	$j = 2$	$j = 3$	$j = 4$	$j = 5$	$j = 6$	$j = 7$	$j = 8$
$i = 2$	0.941							
	(0.016)							
$i = 3$	0.971	0.987						
	(0.011)	(0.007)						
$i = 4$	0.968	0.962	0.961					
	(0.010)	(0.016)	(0.012)					
$i = 5$	0.984	0.997	0.975	0.997				
	(0.005)	(0.002)	(0.013)	(0.002)				
$i = 6$	0.994	0.976	0.958	0.970	0.984			
	(0.003)	(0.010)	(0.015)	(0.012)	(0.007)			
$i = 7$	0.993	0.996	0.917	0.993	0.985	0.986		
	(0.005)	(0.005)	(0.045)	(0.004)	(0.006)	(0.011)		
$i = 8$	0.958	0.964	0.978	0.975	0.991	0.979	0.983	
	(0.031)	(0.030)	(0.010)	(0.011)	(0.004)	(0.007)	(0.037)	
$i = 9$	0.993	0.484	0.943	0.989	0.979	0.995	0.965	0.990
	(0.005)	(0.146)	(0.070)	(0.007)	(0.013)	(0.005)	(0.016)	(0.005)

Table 15

Posterior means (standard deviation) of $\boldsymbol{\xi}^*$: U.S. stock returns. CRSV model.

ξ_{ij}	$j = 1$	$j = 2$	$j = 3$	$j = 4$	$j = 5$	$j = 6$	$j = 7$	$j = 8$
$i = 2$	−0.0431							
	(0.0161)							
$i = 3$	−0.0013	−0.0682						
	(0.0120)	(0.0173)						
$i = 4$	−0.0250	0.0321	0.0668					
	(0.0115)	(0.0180)	(0.0147)					
$i = 5$	−0.0724	0.0398	0.0168	−0.1304				
	(0.0132)	(0.0167)	(0.0249)	(0.0183)				
$i = 6$	−0.1736	0.0253	0.0374	−0.0109	0.0123			
	(0.0195)	(0.0089)	(0.0147)	(0.0224)	(0.0139)			
$i = 7$	−0.0361	0.0315	0.0299	0.0291	−0.0504	0.0088		
	(0.0107)	(0.0066)	(0.0136)	(0.0194)	(0.0092)	(0.0135)		
$i = 8$	−0.0264	0.0044	0.0173	0.0298	−0.0013	−0.0524	0.0014	
	(0.0080)	(0.0231)	(0.0174)	(0.0160)	(0.0073)	(0.0107)	(0.0196)	
$i = 9$	−0.0023	0.0444	0.0085	−0.0387	0.0099	0.0032	0.0329	0.0380
	(0.0096)	(0.0179)	(0.0164)	(0.0145)	(0.0098)	(0.0052)	(0.0120)	(0.0083)

should be treated as equally important. Engle and Colacito (2006) proposed the model comparison based on the variances of portfolios given the expected returns. Univariate loss functions may be used for such a comparison of variances of portfolios. In this section, we compare the forecasting performance by using the three portfolio strategies: (1) minimum-variance strategy, (2) mean-variance strategy, and (3) maximum-expected return strategy (see, *e.g.* Han, 2006) for three multivariate SV models: CSV model, CRSV model without leverage (by setting $\mathbf{R} = \mathbf{O}$ and $\mathbf{S} = \mathbf{I}$) and CRSV model.

Predictive mean and covariance. The procedures for volatility forecasting are as follows. We first estimate parameters using 1742 ($n = 1,742$) observations from February 1, 2001 to January 8, 2008, and forecast the volatility for January 9, 2008. We then shift the sample period one day (from February 2, 2001 to January 9, 2008) to estimate parameters and forecast the volatility for January 10, 2008. We continue this one-day ahead forecast by rolling the sample period until we forecast the volatility for December 31, 2009, which results in 500 one-day ahead forecasts.

Table 16
Posterior means (standard deviation) of $\mathbf{C}^*$: U.S. stock returns. CRSV model.

$\sigma_{u,ij}$	$j=1$	$j=2$	$j=3$	$j=4$	$j=5$	$j=6$	$j=7$	$j=8$
$i=2$	0.126							
	(0.002)							
$i=3$	0.134	0.182						
	(0.002)	(0.003)						
$i=4$	0.138	0.179	0.151					
	(0.002)	(0.003)	(0.002)					
$i=5$	0.202	0.272	0.231	0.245				
	(0.003)	(0.004)	(0.003)	(0.004)				
$i=6$	0.150	0.208	0.178	0.189	0.123			
	(0.002)	(0.003)	(0.002)	(0.003)	(0.002)			
$i=7$	0.140	0.195	0.153	0.173	0.116	0.162		
	(0.002)	(0.003)	(0.002)	(0.002)	(0.002)	(0.002)		
$i=8$	0.124	0.183	0.153	0.175	0.103	0.139	0.150	
	(0.002)	(0.003)	(0.002)	(0.003)	(0.002)	(0.002)	(0.001)	
$i=9$	0.114	0.142	0.126	0.140	0.092	0.130	0.130	0.138
	(0.001)	(0.006)	(0.002)	(0.002)	(0.001)	(0.002)	(0.002)	(0.002)

Table 17
Posterior means (standard deviation) of $\mathbf{D}^*$: U.S. stock returns. CRSV model.

τ_{ij}	$j=1$	$j=2$	$j=3$	$j=4$	$j=5$	$j=6$	$j=7$	$j=8$
$i=2$	0.0283							
	(0.0041)							
$i=3$	0.0143	0.0198						
	(0.0028)	(0.0042)						
$i=4$	0.0177	0.0205	0.0220					
	(0.0027)	(0.0046)	(0.0035)					
$i=5$	0.0119	0.0097	0.0123	0.0132				
	(0.0018)	(0.0019)	(0.0038)	(0.0026)				
$i=6$	0.0125	0.0117	0.0127	0.0232	0.0062			
	(0.0017)	(0.0027)	(0.0029)	(0.0051)	(0.0014)			
$i=7$	0.0048	0.0062	0.0182	0.0098	0.0093	0.0072		
	(0.0011)	(0.0022)	(0.0065)	(0.0018)	(0.0018)	(0.0027)		
$i=8$	0.0071	0.0097	0.0088	0.0181	0.0044	0.0070	0.0101	
	(0.0025)	(0.0045)	(0.0022)	(0.0040)	(0.0007)	(0.0014)	(0.0018)	
$i=9$	0.0042	0.0512	0.0069	0.0082	0.0040	0.0034	0.0077	0.0057
	(0.0010)	(0.0151)	(0.0028)	(0.0020)	(0.0010)	(0.0013)	(0.0017)	(0.0012)

Let N denote the number of MCMC iterations used in the parameter estimation, and $(\boldsymbol{\theta}^{(i)}, \{\boldsymbol{h}_t^{(i)}\}_{t=1}^n, \{\boldsymbol{h}_t^{*(i)}\}_{t=1}^n, \{\boldsymbol{m}_t^{(i)}\}_{t=1}^n)$ denote the MCMC sample of $(\boldsymbol{\theta}, \{\boldsymbol{h}_t\}_{t=1}^n, \{\boldsymbol{h}_t^*\}_{t=1}^n, \{\boldsymbol{m}_t\}_{t=1}^n)$ at the ith iteration $(i = 1, \ldots, N)$. Further, let $\boldsymbol{m}_{t+1|t} \equiv E[\boldsymbol{y}_{t+1}|\mathcal{F}_t]$ and $\boldsymbol{\Sigma}_{t+1|t} \equiv Var[\boldsymbol{y}_{t+1}|\mathcal{F}_t]$ denote the conditional mean and covariance of stock returns $\boldsymbol{y}_{t+1}$, given the current information set $\mathcal{F}_t$ at time t. Then, the one-step-ahead volatility forecast is obtained by adding the following several steps to each MCMC iteration:

1. Generate $\boldsymbol{h}_{n+1}^{(i)}, \boldsymbol{h}_{n+1}^{*(i)}, \boldsymbol{m}_{n+1}^{(i)}|\{\boldsymbol{z}_t\}_{t=1}^n, \boldsymbol{\theta}^{(i)}, \{\boldsymbol{h}_t^{(i)}\}_{t=1}^n, \{\boldsymbol{h}_t^{*(i)}\}_{t=1}^n, \{\boldsymbol{m}_t^{(i)}\}_{t=1}^n$.
2. Store

$$\mathbf{V}_{n+1|n}^{(i)} = \text{diag}\big(\exp(h_{11,n+1}^{(i)}), \exp(h_{22,n+1}^{(i)}), \ldots, \exp(h_{pp,n+1}^{(i)})\big),$$

$$\mathbf{H}_{n+1|n}^{*(i)} = \begin{pmatrix} 1 & 0 & 0 & \cdots & 0 \\ -h_{21,n+1}^{(i)} & 1 & 0 & \cdots & 0 \\ -h_{31,n+1}^{(i)} & -h_{32,n+1}^{(i)} & 1 & \ddots & \vdots \\ \vdots & \vdots & \ddots & \ddots & 0 \\ -h_{p1,n+1}^{(i)} & -h_{p2,n+1}^{(i)} & \cdots & -h_{p\,p-1,n+1}^{(i)} & 1 \end{pmatrix},$$

$$\boldsymbol{\Omega}_m^{(i)} = \text{diag}(\sigma_{m1}^{2(i)}, \ldots, \sigma_{mp}^{2(i)}),$$

to compute the posterior predictive means of $\boldsymbol{m}_{n+1|n}$ and $\boldsymbol{\Sigma}_{n+1|n}$ given by

$$\hat{\boldsymbol{m}}_{n+1|n} = \frac{1}{N}\sum_{i=1}^N \boldsymbol{m}_{n+1|n}^{(i)},$$
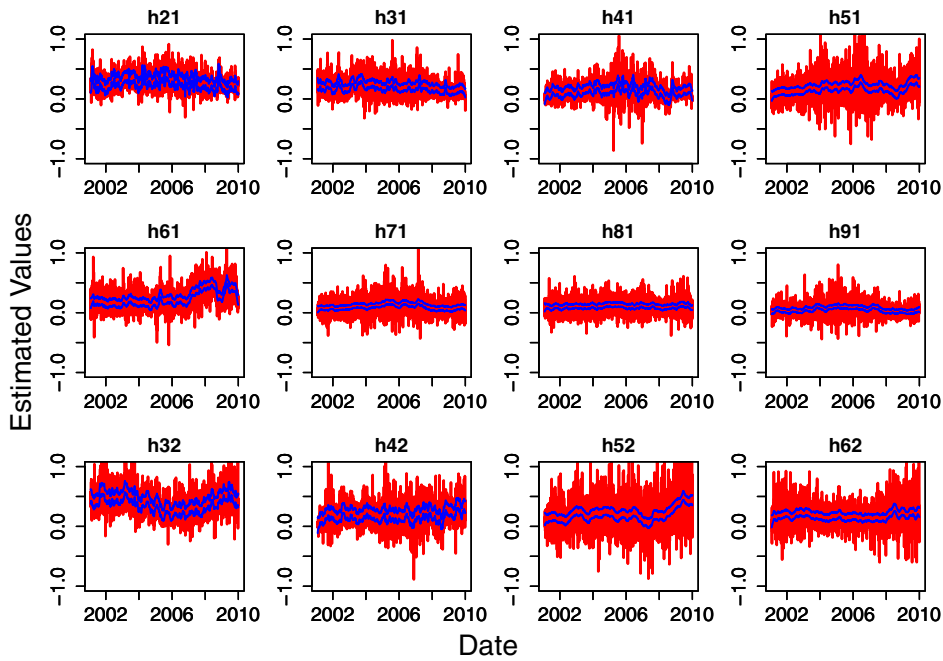
Fig. 6. 95% credible intervals (blue) for $\xi_{21}^* + h_{21,t}, \ldots, \xi_{62}^* + h_{62,t}$, and $x_{21,t}^*, \ldots, x_{62,t}^*$ (red). (For interpretation of the references to color in this figure legend, the reader is referred to the web version of this article.)
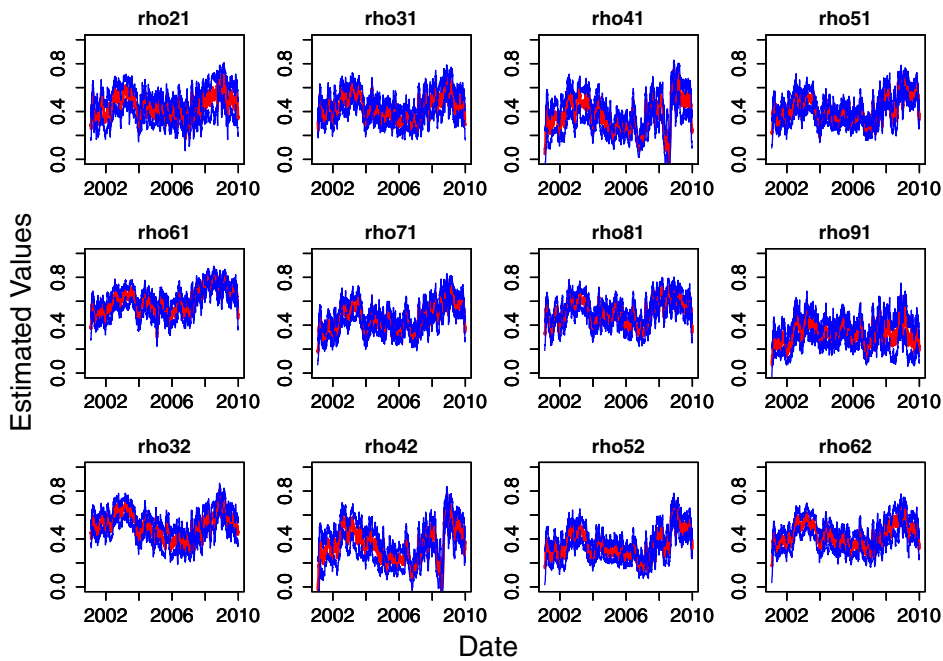
Fig. 7. Posterior means (red) and 95% credible intervals (blue) for $\rho_{21,t}, \ldots, \rho_{62,t}$. (For interpretation of the references to color in this figure legend, the reader is referred to the web version of this article.)

$$\hat{\boldsymbol{\Sigma}}_{n+1|n} = \frac{1}{N} \sum_{i=1}^{N} \boldsymbol{\Sigma}_{n+1|n}^{(i)} = \frac{1}{N} \sum_{i=1}^{N} \left(\mathbf{H}_{n+1|n}^{*-1(i)} \mathbf{V}_{n+1|n}^{(i)} \mathbf{H}_{n+1|n}^{*-1'(i)} + \boldsymbol{\Omega}_{m}^{(i)} \right).$$

We set $N = 3000$ with the burn-in period of 1000 for each one-step-ahead prediction. The initial values for parameters and latent variables are set to their posterior means of previous MCMC iteration.

Portfolio performance. We describe three strategies: (1) minimum-variance strategy, (2) mean-variance strategy, and (3) maximum-expected return strategy. Let $\mu_{p,t+1}$ and $\sigma^2_{p,t+1}$ denote the conditional mean and variance of the portfolio returns, $r_{p,t+1}$, and let r_f denote the risk-free asset return where we use the federal funds rate for r_f. If we let $\boldsymbol{\omega}_t$ denote the vector of portfolio weights for stock returns, then

$$\mu_{p,t+1} = \boldsymbol{\omega}_t' \boldsymbol{m}_{t+1|t} + (1 - \boldsymbol{\omega}_t' \boldsymbol{1}_p) r_f,$$
$$\sigma^2_{p,t+1} = \boldsymbol{\omega}_t' \boldsymbol{\Sigma}_{t+1|t} \boldsymbol{\omega}_t.$$

- *Minimum-variance strategy*

  This strategy is to minimize the conditional variance $\sigma^2_{p,t+1}$ for given levels of conditional expected return $\mu_{p,t+1} = \mu^*_p$. The investors solve the following quadratic problem at time t:

  $$\min_{\boldsymbol{\omega}_t} \sigma^2_{p,t+1} \quad \text{s.t.} \quad \mu^2_{p,t+1} = \mu^*_p,$$

  where μ^*_p is the target expected return. The solution is

  $$\hat{\boldsymbol{\omega}}_t = \boldsymbol{\Sigma}^{-1}_{t+1|t} (\boldsymbol{m}_{t+1|t} - r_f \boldsymbol{1}_p) \frac{\mu^*_p - r_f}{\kappa_t},$$
  $$\kappa_t = (\boldsymbol{m}_{t+1|t} - r_f \boldsymbol{1}_p)' \boldsymbol{\Sigma}^{-1}_{t+1|t} (\boldsymbol{m}_{t+1|t} - r_f \boldsymbol{1}_p).$$

- *Mean-variance strategy*

  This strategy is to maximize an expected mean-variance utility function. The investors then solve the following utility maximization problem,

  $$\max_{\boldsymbol{w}_t} \left\{ \mu_{p,t+1} - \frac{\gamma}{2} \sigma^2_{p,t+1} \right\},$$

  where γ is the coefficient of the absolute risk aversion. The high value of the risk aversion γ implies that people tend to be risk aversive. The solution is

  $$\hat{\boldsymbol{\omega}}_t = \frac{1}{\gamma} \boldsymbol{\Sigma}^{-1}_{t+1|t} (\boldsymbol{m}_{t+1|t} - r_f \boldsymbol{1}_p).$$

  Thus the risk-aversion coefficient γ can influence not to the relative weights of individual risky assets but the sum of their weights.

- *Maximum expected return strategy*

  This strategy is to maximize the conditional expected return $\mu_{p,t+1}$ for a given level of conditional volatility $\sigma^2_{p,t+1} = \sigma^{*2}_p$. The investors solve the following problem at time t:

  $$\max_{\boldsymbol{\omega}_t} \mu_{p,t+1} \quad \text{s.t} \quad \sigma^2_{p,t+1} = \sigma^{*2}_p,$$

  where σ^{*2}_p the target level of variance. The solution is given by

  $$\hat{\boldsymbol{\omega}}_t = \boldsymbol{\Sigma}^{-1}_{t+1|t} (\boldsymbol{m}_{t+1|t} - r_f \boldsymbol{1}_p) \sqrt{\frac{\sigma^{*2}_p}{\kappa_t}},$$
  $$\kappa_t = (\boldsymbol{m}_{t+1|t} - r_f \boldsymbol{1}_p)' \boldsymbol{\Sigma}^{-1}_{t+1|t} (\boldsymbol{m}_{t+1|t} - r_f \boldsymbol{1}_p).$$

Estimation results

The cumulative objective functions (realized variances, realized utility functions and realized returns) are shown in Table 18 for (1) minimum-variance strategy with $\mu^*_p = 0.004$, 0.01 and 0.1, (2) mean-variance strategy with $\gamma = 6$, 10 and 15, and (3) maximum-return strategy with $\sigma^*_p = 0.001$, 0.01 and 0.1 for CSV and CRSV models.

We also include a simple benchmark model that is based on the exponentially weighted moving average (EWMA) approach for forecasting covariance matrices of assets by incorporating realized covariance matrices as follows:

$$\boldsymbol{\Sigma}_{t+1|t} = \lambda \boldsymbol{\Sigma}_{t|t-1} + (1 - \lambda) \mathbf{RC}_t, \tag{19}$$

where λ is a decay factor and three decay factors are considered, namely, $\lambda = 0.90$, 0.95 and 0.98. With regard to the specification of the mean of asset returns, we use the sample mean of asset returns, i.e., $\boldsymbol{m}_{t+1|t} = \frac{1}{t} \sum_{s=1}^{t} \boldsymbol{y}_s$.

For the minimum-variance strategy, CRSV models outperform CSV and EWMA models, and CRSV models with and without leverage perform equally well. For the mean-variance strategy, CSV and CRSV models outperform EWMA models, and there is little difference between the two best models (CSV and CRSV with leverage models). For maximum-return strategies, CRSV model with leverage outperforms CSV, CRSV without leverage, and EWMA models. Overall, CRSV models outperform other models, while the performances of the simple benchmark (EWMA) models are poor.

Figs. 8–10 show the time-series plots of the weight for the ith stock, ω_{it}, for three strategies in CRSV models. Under the riskiest settings in each strategy (i.e., $\mu^*_p = 0.1, \gamma = 6, \sigma^*_p = 0.1$), it is found that the portfolio weights fluctuate more drastically than those under two other less risky settings in each strategy during the prediction period. We also note that

Table 18
The value of cumulative objective functions for three strategies: bold font means highest performance among models.

Minimum-Variance	$\mu_p^*=0.004$	$\mu_p^*=0.01$	$\mu_p^*=0.1$
EWMA ($\lambda = 0.90$)	3.041	17.04	3135
EWMA ($\lambda = 0.95$)	3.073	18.12	3182
EWMA ($\lambda = 0.98$)	3.160	18.75	3284
CSV	2.108	12.88	1976
CRSV ($\mathbf{R} = \mathbf{O}, \mathbf{S} = \mathbf{I}$)	0.751	**4.218**	**712.4**
CRSV	**0.748**	4.448	730.4
Mean-Variance	$\gamma = 6$	$\gamma = 10$	$\gamma = 15$
EWMA ($\lambda = 0.90$)	0.698	0.983	1.126
EWMA ($\lambda = 0.95$)	0.738	1.007	1.142
EWMA ($\lambda = 0.98$)	0.861	1.081	1.191
CSV	**1.073**	**1.208**	**1.276**
CRSV ($\mathbf{R} = \mathbf{O}, \mathbf{S} = \mathbf{I}$)	0.769	1.025	1.154
CRSV	0.981	1.153	1.239
Maximum-Return	$\sigma_p^{*2} = 0.001$	$\sigma_p^{*2} = 0.01$	$\sigma_p^{*2} = 0.1$
EWMA ($\lambda = 0.90$)	-0.751	-5.428	-20.21
EWMA ($\lambda = 0.95$)	-0.721	-5.332	-19.91
EWMA ($\lambda = 0.98$)	-0.467	-4.530	-17.37
CSV	1.124	0.511	-1.427
CRSV ($\mathbf{R} = \mathbf{O}, \mathbf{S} = \mathbf{I}$)	1.142	0.569	-1.243
CRSV	**1.172**	**0.662**	**-0.947**

*For example, for the maximum-return strategy, the cumulative realized returns are computed as $\sum_{t=1742}^{2241}\{\hat{\omega}_t' \mathbf{y}_{t+1} + (1 - \hat{\omega}_t' \mathbf{1}_p)r_f\}$ where $\hat{\omega}_t$ is the vector of portfolio weights estimated at time t.
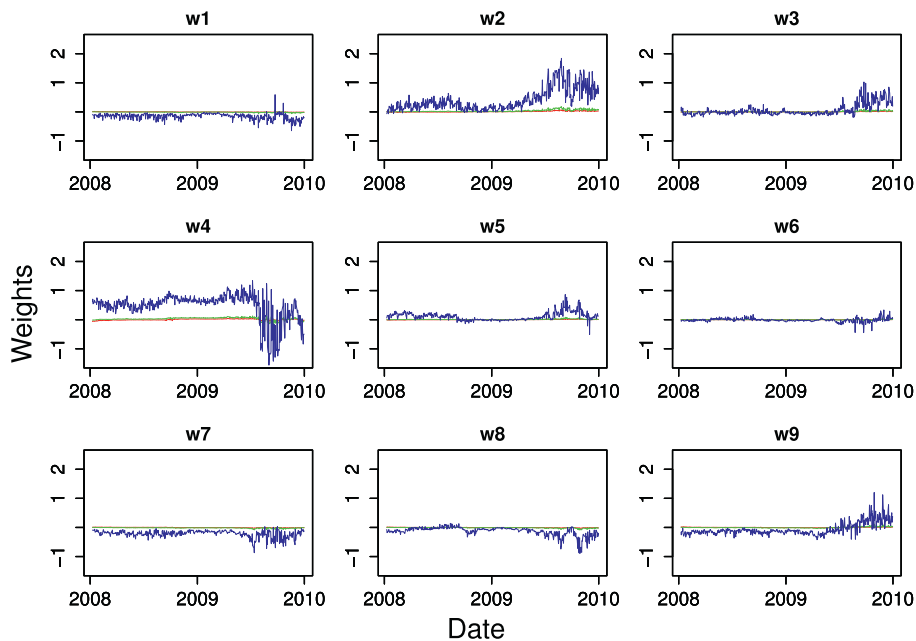
Fig. 8. Time series plot of the portfolio weight ω_{it} for minimum-variance strategy: $\mu_p^* = 0.004$ (red), $\mu_p^* = 0.01$ (green) and $\mu_p^* = 0.1$ (blue). CRSV model. (For interpretation of the references to color in this figure legend, the reader is referred to the web version of this article.)

the weights for the mean-variance strategy do not change so much during the prediction period, and the weights for the risk-free asset are more than 95% weight under all levels of the risk aversion. Furthermore, the weights for the maximum-return strategy take more stable values relatively than those for the minimum-variance strategy.

Furthermore, Fig. 14 illustrates the cumulative realized return for the three models. Since the weighs for risk assets under the mean-variance strategy are close to zero, the differences in cumulative realized returns among the three models are very small for this strategy. For the minimum-variance and the maximum-return strategies, the CSV model demonstrates a higher performance from the end of 2008 to the middle of 2009 than other two models, but its performance fluctuates drastically during the prediction period. In contrast, CRSV models show more stable performance during the period.
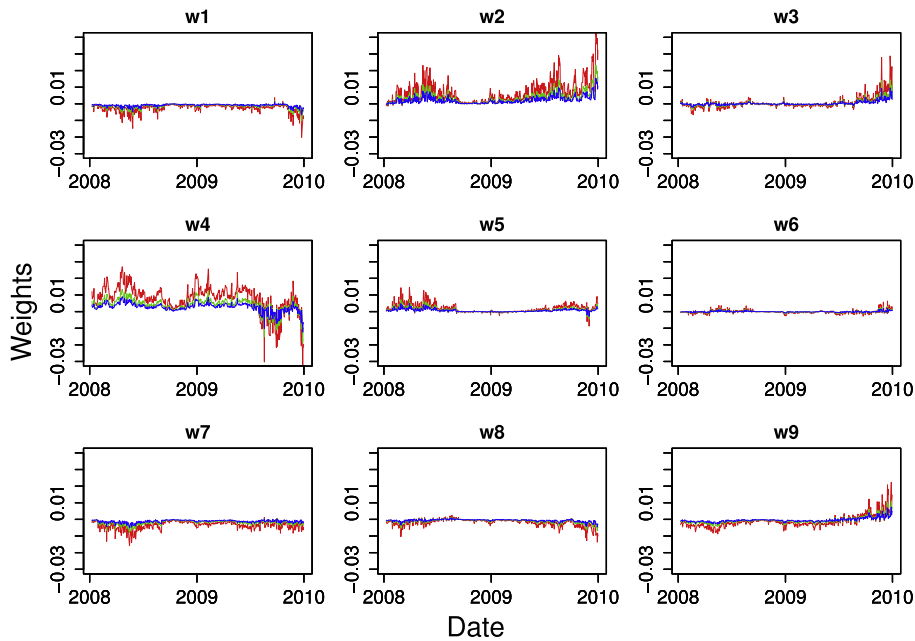
Fig. 9. Time series plot of the portfolio weight ω_{it} for mean-variance strategy: $\gamma = 6$ (red), $\gamma = 10$ (green) and $\gamma = 15$ (blue). CRSV model. (For interpretation of the references to color in this figure legend, the reader is referred to the web version of this article.)

Fig. 10. Time series plot of the portfolio weight ω_{it} for maximum return strategy: $\sigma_p^{*2} = 0.001$ (red), $\sigma_p^{*2} = 0.01$ (green) and $\sigma_p^{*2} = 0.1$ (blue). CRSV model. (For interpretation of the references to color in this figure legend, the reader is referred to the web version of this article.)

6. Conclusion

In this paper, we propose the CRSV model that are simultaneous models of multiple daily asset returns and realized covariance, where the well-known bias problems in realized measures due to market microstructure noise and nontrading hours are automatically solved within our proposed framework. Furthermore, we extend these models to incorporate the leverage effects that have been observed in the literature in univariate SV models. By using the Bayesian approach, the efficient MCMC algorithm is described for the parameter estimation. In our empirical studies, our proposed CRSV models capture the dynamic behaviors of diagonal and off-diagonal components of Cholesky-decomposed covariance matrices and
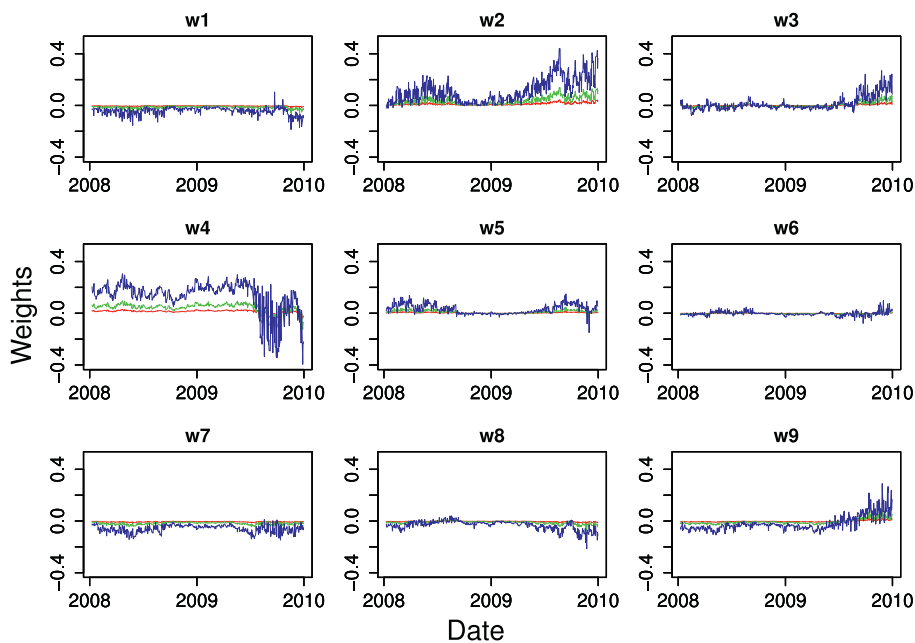
Fig. 11. Time series plot of the portfolio weight ω_{it} for minimum-variance strategy: $\mu_p^* = 0.004$ (red) and $\mu_p^* = 0.01$ (green). CRSV model. (For interpretation of the references to color in this figure legend, the reader is referred to the web version of this article.)
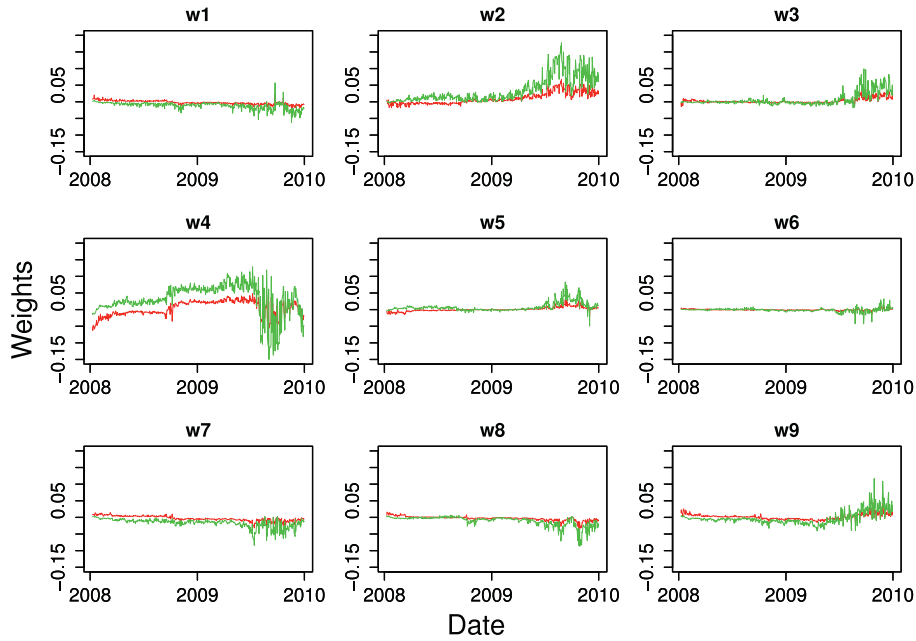

Fig. 12. Time series plot of the portfolio weight ω_{it} for mean-variance strategy: $\gamma = 10$ (green) and $\gamma = 15$ (blue). CRSV model. (For interpretation of the references to color in this figure legend, the reader is referred to the web version of this article.)

outperform CSV models. The dynamic leverage effects **R** and the correlation matrix **S** for $\boldsymbol{h}_{t+1}$ given $\boldsymbol{y}_t$ are shown to improve the portfolio performances. Furthermore, the cumulative returns for CRSV models are less volatile than those of the CSV model.

In our future work, we could consider several directions. First, more parsimonious modeling by detecting the sparsity of off-diagonal components may improve the forecasting performances of the multivariate SV model by using, for example, Bayesian threshold dynamic modeling (Nakajima and West, 2013a, 2013b). Second, the long memory property of diagonal
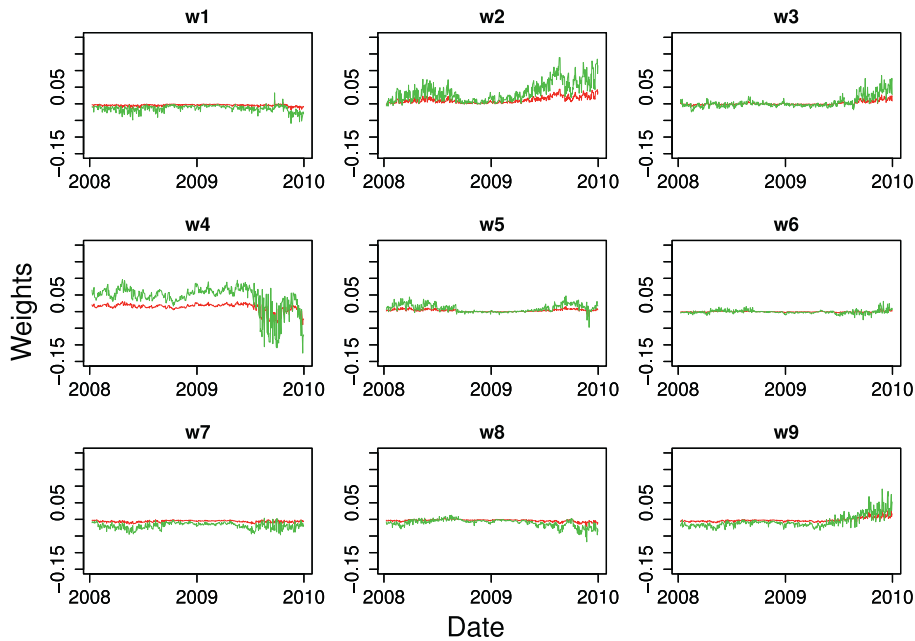
Fig. 13. Time series plot of the portfolio weight ω_{it} for maximum return strategy: $\sigma_p^{*2} = 0.001$ (red) and $\sigma_p^{*2} = 0.01$ (green). CRSV model. (For interpretation of the references to color in this figure legend, the reader is referred to the web version of this article.)
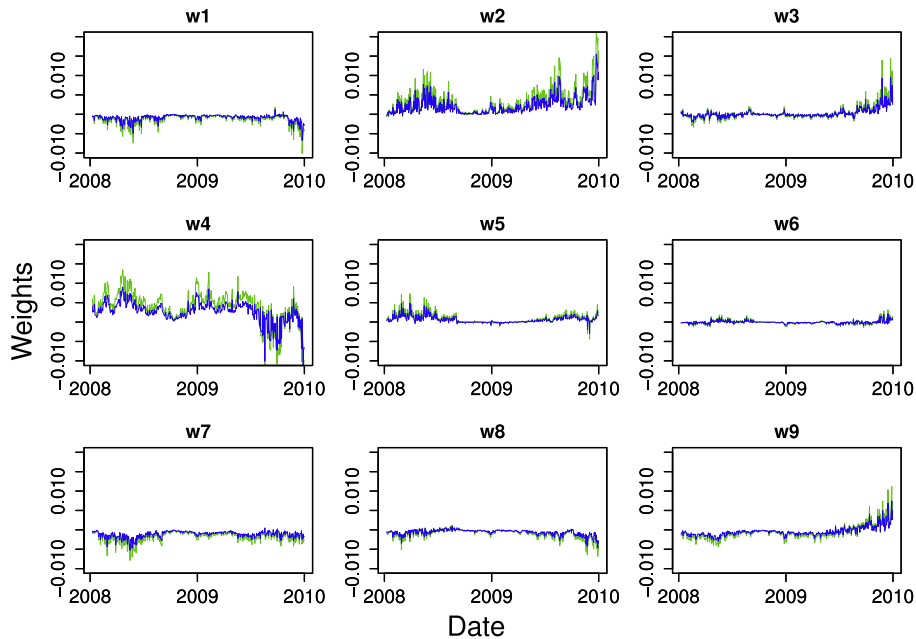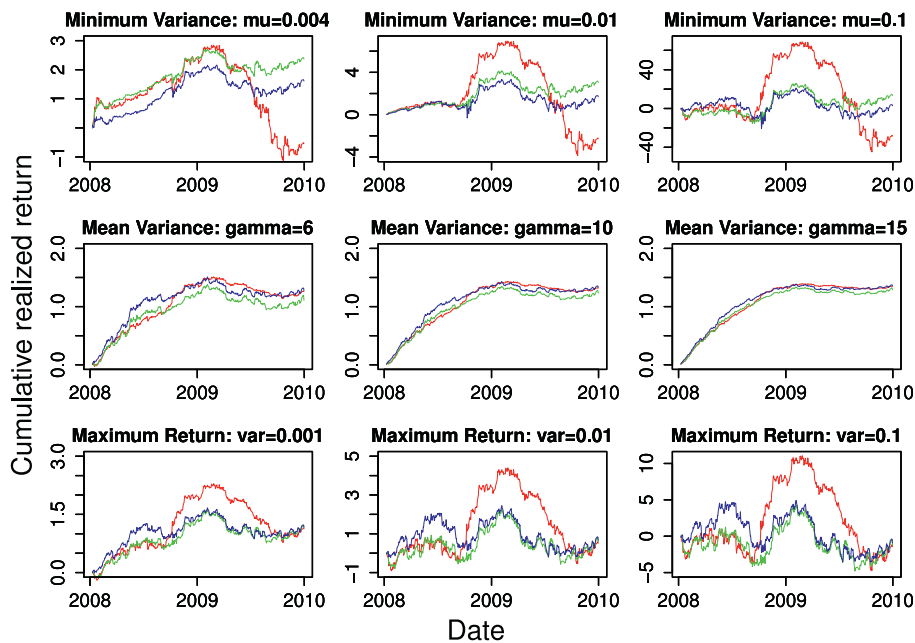

Fig. 14. Cumulative realized return: red (CSV), green (CRSV ($\mathbf{R} = \mathbf{O}, \mathbf{S} = \mathbf{I}$)) and blue (CRSV). (For interpretation of the references to color in this figure legend, the reader is referred to the web version of this article.)

components may be considered. Since the realized volatilities are well known to have high persistence, a superposition model can be used to describe such long-range dependence and to improve the goodness of fit to the data. Finally, although our specification of stock returns is a simple random walk process, more sophisticated mean structures such as factor SV models may be useful to improve the portfolio performances.

Fig. 15. Realized portfolio variance $\hat{\omega}_t'\hat{\Sigma}_t\hat{\omega}_t$, where $\hat{\Sigma}_t$ is realized covariance at time t: red (CSV), green (CRSV ($\mathbf{R} = \mathbf{O}, \mathbf{S} = \mathbf{I}$)) and blue (CRSV). (For interpretation of the references to color in this figure legend, the reader is referred to the web version of this article.)

Acknowledgments
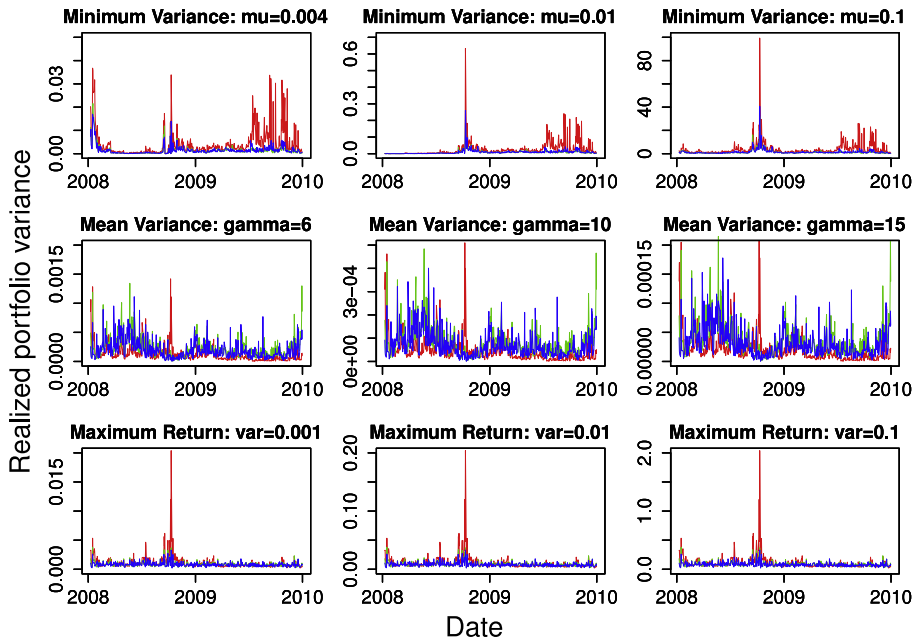
Appendix A. The details of MCMC algorithm

A1. Generation of $(\xi, \boldsymbol{\xi}^*, \boldsymbol{\mu}, \boldsymbol{\mu}^*)$

We assume that prior distributions are

$$\xi \sim \mathcal{N}(\xi_0, \sigma_{\xi 0}^2), \quad \boldsymbol{\xi}^* \sim \mathcal{N}(\boldsymbol{\xi}_0^*, \boldsymbol{\Xi}_0^*), \quad \boldsymbol{\mu} \sim \mathcal{N}(\boldsymbol{\mu}_0, \tilde{\mathbf{M}}_0), \quad \boldsymbol{\mu}^* \sim \mathcal{N}(\boldsymbol{\mu}_0^*, \tilde{\mathbf{M}}_0^*).$$

Then the conditional posterior distributions of $(\xi, \boldsymbol{\xi}^*, \boldsymbol{\mu}, \boldsymbol{\mu}^*)$ are independent given other parameters, $\boldsymbol{m}$, $\boldsymbol{h}$ and $\boldsymbol{h}^*$. The posterior distributions are

$$\xi \sim \mathcal{N}(\xi_1, \sigma_{\xi 1}^2), \quad \boldsymbol{\xi}^* \sim \mathcal{N}(\boldsymbol{\xi}_1^*, \boldsymbol{\Xi}_1^*), \quad \boldsymbol{\mu} \sim \mathcal{N}(\boldsymbol{\mu}_1, \tilde{\mathbf{M}}_1), \quad \boldsymbol{\mu}^* \sim \mathcal{N}(\boldsymbol{\mu}_1^*, \tilde{\mathbf{M}}_1^*),$$

where

$$\sigma_{\xi 1}^{-2} = \sigma_{\xi 0}^{-2} + n\mathbf{1}_p'\mathbf{C}^{-1}\mathbf{1}_p, \quad \xi_1 = \sigma_{\xi 1}^2\left\{\sigma_{\xi 0}^{-2}\xi_0 + \mathbf{1}_p'\mathbf{C}^{-1}\sum_{t=1}^n(\boldsymbol{x}_t - \boldsymbol{h}_t)\right\},$$

$$\boldsymbol{\Xi}_1^{*-1} = \boldsymbol{\Xi}_0^{*-1} + n\mathbf{C}^{*-1}, \quad \boldsymbol{\xi}_1^* = \boldsymbol{\Xi}_1^*\left\{\boldsymbol{\Xi}_0^{*-1}\boldsymbol{\xi}_0^* + \mathbf{C}^{*-1}\sum_{t=1}^n(\boldsymbol{x}_t^* - \boldsymbol{h}_t^*)\right\},$$

and

$$\tilde{\mathbf{M}}_1^{-1} = \tilde{\mathbf{M}}_0^{-1} + (n-1)(\mathbf{I}_p - \boldsymbol{\Phi})\mathbf{S}'\mathbf{D}^{-1}\mathbf{S}(\mathbf{I}_p - \boldsymbol{\Phi}) + \lambda^{-1}\mathbf{S}'\mathbf{D}^{-1}\mathbf{S},$$

$$\boldsymbol{\mu}_1 = \tilde{\mathbf{M}}_1\left[\tilde{\mathbf{M}}_0^{-1}\boldsymbol{\mu}_0 + (\mathbf{I}_p - \boldsymbol{\Phi})\mathbf{S}'\mathbf{D}^{-1}\mathbf{S}\sum_{t=1}^{n-1}\left\{\boldsymbol{h}_{t+1} - \boldsymbol{\Phi}\boldsymbol{h}_t - \mathbf{R}\mathbf{V}_t^{-1/2}\mathbf{H}_t^*(\boldsymbol{y}_t - \boldsymbol{m}_t)\right\} + \lambda^{-1}\mathbf{S}'\mathbf{D}^{-1}\mathbf{S}\boldsymbol{h}_1\right],$$

$$\tilde{\mathbf{M}}_1^{*-1} = \tilde{\mathbf{M}}_0^{*-1} + (n-1)(\mathbf{I}_K - \boldsymbol{\Phi}^*)\mathbf{D}^{-1}(\mathbf{I}_k - \boldsymbol{\Phi}^*) + \lambda^{*-1}\mathbf{D}^{-1},$$

$$\boldsymbol{\mu}_1^* = \tilde{\mathbf{M}}_1^*\left[\tilde{\mathbf{M}}_0^{*-1}\boldsymbol{\mu}_0^* + (\mathbf{I}_K - \boldsymbol{\Phi}^*)\mathbf{D}^{-1}\sum_{t=1}^{n-1}\left(\boldsymbol{h}_{t+1}^* - \boldsymbol{\Phi}^*\boldsymbol{h}_t^*\right) + \lambda^{*-1}\mathbf{D}^{-1}\boldsymbol{h}_1^*\right].$$

A2. Generation of $\boldsymbol{\phi}$ and $\boldsymbol{\phi}^*$

Given other parameters and variables, $\boldsymbol{\phi}$ and $\boldsymbol{\phi}^*$ are conditionally independent. For the prior distribution of $\boldsymbol{\phi}$, we assume $(\phi_i + 1)/2 \sim \mathcal{B}(a_{0i}, b_{0i})$ for $i = 1, \ldots, p$, and denote the prior probability density function by $\pi(\boldsymbol{\phi})$. Then

$$\log \pi(\boldsymbol{\phi}|\boldsymbol{\theta}_{\backslash \boldsymbol{\phi}, \boldsymbol{\phi}^*}, \boldsymbol{m}, \boldsymbol{h}, \boldsymbol{h}^*, \boldsymbol{z}) = \text{const.} + \log \pi(\boldsymbol{\phi}) - (\boldsymbol{\phi} - \boldsymbol{\mu}_{\boldsymbol{\phi}})' \boldsymbol{\Sigma}_{\boldsymbol{\phi}}^{-1}(\boldsymbol{\phi} - \boldsymbol{\mu}_{\boldsymbol{\phi}}),$$

where

$$\boldsymbol{\Sigma}_{\boldsymbol{\phi}}^{-1} = (\mathbf{S}'\mathbf{D}^{-1}\mathbf{S}) \odot \left\{ \sum_{t=1}^{n-1} (\boldsymbol{h}_t - \boldsymbol{\mu})(\boldsymbol{h}_t - \boldsymbol{\mu})' \right\}, \quad \boldsymbol{\mu}_{\boldsymbol{\phi}} = \boldsymbol{\Sigma}_{\boldsymbol{\phi}} \boldsymbol{b}_{\boldsymbol{\phi}}, \tag{20}$$

and $\boldsymbol{b}_{\boldsymbol{\phi}}$ is the column vector with diagonal elements of

$$\mathbf{S}'\mathbf{D}^{-1}\mathbf{S} \sum_{t=1}^{n-1} \left\{ \boldsymbol{h}_{t+1} - \boldsymbol{\mu} - \mathbf{RV}_t^{-1/2} \mathbf{H}_t^*(\boldsymbol{y}_t - \boldsymbol{m}_t) \right\} (\boldsymbol{h}_t - \boldsymbol{\mu})'.$$

We generate a candidate $\boldsymbol{\phi}^\dagger$ from a truncated multivariate normal distribution $\mathcal{TN}_{R_{\boldsymbol{\phi}}}(\boldsymbol{\mu}_{\boldsymbol{\phi}}, \boldsymbol{\Sigma}_{\boldsymbol{\phi}})$ where $R_{\boldsymbol{\phi}} = \{\boldsymbol{\phi}| \; |\phi_i| < 1, i = 1, \ldots, p\}$ and accept it with probability $\min\{1, \pi(\boldsymbol{\phi}^\dagger)/\pi(\boldsymbol{\phi})\}$.

Let $\pi(\boldsymbol{\phi}^*)$ denote the prior probability density function of $\boldsymbol{\phi}^*$. Then

$$\log \pi(\boldsymbol{\phi}^*|\boldsymbol{\theta}_{\backslash \boldsymbol{\phi}, \boldsymbol{\phi}^*}, \boldsymbol{m}, \boldsymbol{h}, \boldsymbol{h}^*, \boldsymbol{z}) = \text{const.} + \log \pi(\boldsymbol{\phi}^*) - (\boldsymbol{\phi}^* - \boldsymbol{\mu}_{\boldsymbol{\phi}^*})' \boldsymbol{\Sigma}_{\boldsymbol{\phi}^*}^{-1}(\boldsymbol{\phi}^* - \boldsymbol{\mu}_{\boldsymbol{\phi}^*}),$$

where

$$\boldsymbol{\Sigma}_{\boldsymbol{\phi}^*}^{-1} = \mathbf{D}^{*-1} \odot \left\{ \sum_{t=1}^{n-1} (\boldsymbol{h}_t^* - \boldsymbol{\mu}^*)(\boldsymbol{h}_t^* - \boldsymbol{\mu}^*)' \right\}, \quad \boldsymbol{\mu}_{\boldsymbol{\phi}^*} = \boldsymbol{\Sigma}_{\boldsymbol{\phi}^*} \boldsymbol{b}_{\boldsymbol{\phi}}^*, \tag{21}$$

and $\boldsymbol{b}_{\boldsymbol{\phi}}^*$ is the column vector with diagonal elements of

$$\mathbf{D}^{*-1} \sum_{t=1}^{n-1} \left(\boldsymbol{h}_{t+1}^* - \boldsymbol{\mu}^* \right)(\boldsymbol{h}_t^* - \boldsymbol{\mu}^*)'.$$

When we take a uniform prior on $(-\sqrt{1+\nu}, \sqrt{1+\nu})$, we generate a candidate $\boldsymbol{\phi}^{*\dagger}$ from a truncated multivariate normal distribution $\mathcal{TN}_{R_{\boldsymbol{\phi}^*}}(\boldsymbol{\mu}_{\boldsymbol{\phi}^*}, \boldsymbol{\Sigma}_{\boldsymbol{\phi}^*})$ where $R_{\boldsymbol{\phi}^*} = \{\boldsymbol{\phi}^*| \; |\phi_i^*| < \sqrt{1+\nu}, i = 1, \ldots, K\}$.

A3. Generation of $\mathbf{C}$, $\mathbf{C}^*$, $\mathbf{D}$, $\mathbf{D}^*$ and $\boldsymbol{\Omega}_m$

Note that elements of $\mathbf{C}$, $\mathbf{C}^*$, $\mathbf{D}$, $\mathbf{D}^*$ and $\boldsymbol{\Omega}_m$ are conditionally independent. We assume their prior distributions are

$$\tau_{ij}^2 \sim \mathcal{IG}(a_{\tau,ij}/2, b_\tau/2), \quad \sigma_{u,ij}^2 \sim \mathcal{IG}(a_{u,ij}/2, b_{u,ij}/2), \quad \sigma_{mi}^2 \sim \mathcal{IG}(a_{mi}/2, b_{mi}/2),$$

for $i = 1, \ldots, p$ and $j = 1, \ldots, i$.

In empirical studies, the diagonal components, $\boldsymbol{h}_t$, fluctuate more drastically than off-diagonal components, $\boldsymbol{h}_t^*$. Actually, the time series plots of $\boldsymbol{h}_t^*$ are found to be almost constant or those of the random walk process with small variance. Hence, we shall assume $\mathcal{IG}(\epsilon, \epsilon)$ prior for $\mathbf{D}^*$, ($\tau_{ij}^2, i < j$) with e.g., $\epsilon = 10^{-4}$. Also we expect the variance of the random walk process for the mean vector $\boldsymbol{m}_t$ to be small and hence assume the $\mathcal{IG}(\epsilon, \epsilon)$ prior, with e.g., $\epsilon = 10^{-6}$.

The conditional posterior distributions of τ_{ij}^2's are

$$\tau_{ii}^2|\cdot \sim \mathcal{IG}\left(\frac{a_{\tau,ii} + n}{2}, \frac{b_{\tau,ii} + \sum_{t=1}^n w_{it}^2}{2} \right), \quad \tau_{ij}^2|\cdot \sim \mathcal{IG}\left(\frac{a_{\tau,ij} + n}{2}, \frac{b_{\tau,ij} + \sum_{t=1}^n w_{ij,t}^{*2}}{2} \right),$$

for $i = 1, \ldots, p$ and $j = 1, \ldots, i - 1$, where

$$\boldsymbol{w}_t = \begin{cases} \lambda^{-1/2} \mathbf{S}(\boldsymbol{h}_1 - \boldsymbol{\mu}), & t = 1, \\ \mathbf{S}\{\boldsymbol{h}_t - \boldsymbol{\mu} - \boldsymbol{\Phi}(\boldsymbol{h}_{t-1} - \boldsymbol{\mu}) - \mathbf{RV}_{t-1}^{-1/2} \mathbf{H}_{t-1}^*(\boldsymbol{y}_{t-1} - \boldsymbol{m}_{t-1})\}, & t = 2, \ldots, n, \end{cases}$$

$$w_{ij,t}^* = \begin{cases} \lambda^{*-1/2}(h_{ij,1} - \mu_{ij}), & t = 1, \\ h_{ij,t+1} - \mu_{ij} - \phi_{ij}(h_{ij,t} - \mu_{ij}), & t = 2, \ldots, n. \end{cases}$$

Similarly, the conditional posterior distributions of $\sigma_{u,ij}^2$'s are

$$\sigma_{u,ii}^2|\cdot \sim \mathcal{IG}\left(\frac{a_{u,ii} + n}{2}, \frac{b_{u,ii} + \sum_{t=1}^n (x_{ii,t} - \xi - h_{ii,t})^2}{2} \right),$$

$$\sigma_{u,ij}^2| \cdot \sim \mathcal{IG}\left(\frac{a_{u,ij} + n}{2}, \frac{b_{u,ij} + \sum_{t=1}^{n}(x_{ij,t} - \xi_{ij} - h_{ij,t})^2}{2}\right),$$

for $i = 1, \ldots, p$ and $j = 1, \ldots, i - 1$. Finally, the conditional posterior distributions of σ_{mi}^2's are

$$\sigma_{mi}^2| \cdot \sim \mathcal{IG}\left(\frac{a_{mi} + n}{2}, \frac{b_{mi} + \lambda_m^{-1} m_{i1}^2 + \sum_{t=1}^{n-1}(m_{i,t+1} - m_{it})^2}{2}\right),$$

for $i = 1, \ldots, p$.

References

Aguilar, O., West, M., 2000. Bayesian dynamic factor models and portfolio allocation. J. Bus. Econ. Stat. 18, 338–357.

Andersen, T.G., Bollerslev, T., 1998. Answering the skeptics: Yes, standard volatility models do provide accurate forecasts. Int. Econ. Rev. 39, 885–905.

Asai, M., McAleer, M., 2009. The structure of dynamic correlations in multivariate stochastic volatility models. J. Econom. 150, 182–192.

Barndorff-Nielsen, O.E., Hansen, P.R., Lunde, A., Shephard, N., 2008. Designing realized kernels to measure the ex-post variation of equity prices in the presence of noise. Econometrica 76, 1481–1536.

Barndorff-Nielsen, O.E., Hansen, P.R., Lunde, A., Shephard, N., 2011. Multivariate realized kernels: consistent positive semi-definite estimators of the covariation of equity prices with noise and non-synchronous trading. J. Econom. 162, 149–169.

Barndorff-Nielsen, O.E., Shephard, N., 2001. Non-Gaussian Ornstein-Ulhlenbeck-based models and some of their uses in financial economics. J. R. Stat. Soc., Ser. B 63, 167–241.

Barndorff-Nielsen, O.E., Shephard, N., 2002. Econometric analysis of realized volatility and its use in estimating stochastic volatility models. J. R. Stat. Soc., Ser. B 64, 253–280.

Barndorff-Nielsen, O.E., Shephard, N., 2004. Econometrics analysis of realized covariation: high frequency covariance, regression and correlation in financial ecnomics. Econometrica 72, 885–925.

Bauwens, L., Laurent, S., Rombouts, J.V.K., 2006. Multivariate Garch models: a survey. J. Appl. Econom. 21, 79–109.

Berger, J.O., Yang, R.Y., 1994. Non informative priors and Bayesian testing for the ar(1) model. Econom. Theory 10, 461–482.

Chib, S., 2001. Markov chain monte carlo methods: computation and inference. In: Elliott, G., Granger, C.W.J., Timmermann, A. (Eds.), Handbook of Econometrics, Vol. 5. North Holland Press, Amsterdam, pp. 3569–3649.

Chib, S., Nardari, F., Shephard, N., 2006. Analysis of high dimensional multivariate stochastic volatility models. J. Econom. 134, 341–371.

Dellaportas, P., Pourahmadi, M., 2012. Cholesky-garch models with applications to finance. Stat. Comput. 22, 849–855.

Doornik, J.A., 2009. An Object-Oriented Matrix Programming Language - Ox 6. Timberlake Consultants Press and Oxford, London. www.doornik.com.

Durbin, J., Koopman, S.J., 2002. A simple and efficient simulation smoother for state space time series analysis. Biometrika 89, 603–616.

Engle, R., Colacito, R., 2006. Testing and valuing dynamic correlations for asset allocation. J. Bus. Econ. Stat. 24, 238–253.

Fox, E., Dunson, D., 2015. Bayesian nonparametric covariance regression. J. Mach. Learn. Res.

Geweke, J., Zhou, G., 1996. Measuring the pricing error of the arbitrage pricing theory. Rev. Financ. Stud. 9, 557–587.

Han, Y., 2006. Asset allocation with a high dimensional latent factor stochastic volatility model. Rev. Financ. Stud. 19, 237–271.

Harvey, A.C., Ruiz, E., Shephard, N., 1994. Multivariate stochastic variance models. Rev. Econ. Stud. 61, 247–264.

Heber, G., Lunde, A., Shephard, N., Sheppard, K., 2009. Oxford-Man Institute's Realized Library, version 0.1. Oxford-Man Institute, University of Oxford.

Ishihara, T., Omori, Y., 2012. Efficient bayesian estimation of a multivariate stochastic volatility model with cross leverage and heavy-tailed errors. Comput. Stat. Data Anal. 56, 3674–3689.

Ishihara, T., Omori, Y., Asai, M., 2016. Matrix exponential stochastic volatility with cross leverage. Comput. Stat. Data Anal 100, 331–350.

Jin, X., Maheu, J.M., 2013. Modeling realized covariances and returns. J. Financ. Econ. 11, 335–369.

Jin, X., Maheu, J.M., 2016. Bayesian semiparametric modeling of realized covariance matrices. J. Econom. 192, 19–39.

de Jong, P., Shephard, N., 1995. The simulation smoother for time series models. Biometrika 82, 339–350.

Kim, S., Shephard, N., Chib, S., 1998. Stochastic volatility: likelihood inference and comparison with arch models. Rev. Econ. Studies 65, 361–393.

Koopman, S.J., Scharth, M., 2013. The analysis of stochastic volatility in the presence of daily realized measures. J. Finan. Econom. 76–115.

Liu, J., Maheu, J. M., 2015. Improving Markov Switching Models Using Realized Variance. MPRA Paper No. 71120, (https://mpra.ub.uni-muenchen.de/71120/).

Lopes, H.F., Carvalho, C.M., 2007. Factor stochastic volatility with time varying loadings and Markov switching regimes. J. Stat. Plan. Inference 137, 3082–3091.

Lopes, H. F., McCulloch, R. E., Tsay, R. S., 2014. Parsimony Inducing Priors for Large Scale State-Space Models. Discussion Paper.

Lopes, H.F., West, M., 2004. Bayesian model assessment in factor analysis. Statistica Sinica 14, 41–67.

Lubrano, M., 1995. Testing for unit roots in a Bayesian framework. J. Econom. 69, 81–109.

Nakajima, J., West, M., 2013a. Bayesian analysis of latent threshold dynamic models. J. Bus. Econ. Stat. 31, 151–164.

Nakajima, J., West, M., 2013b. Dynamic factor volatility modeling: A bayesian latent threshold approach. J. Financ. Econ. 11, 116–153.

Noureldin, D., Shephard, N., Sheppard, K., 2012. Multivariate high-frequency-based volatility (heavy) models. J. Appl. Econom. 27, 907–933.

Omori, Y., Chib, S., Shephard, N., Nakajima, J., 2007. Stochastic volatility with leverage: Fast likelihood inference. J. Econom. 140-2, 425–449.

Omori, Y., Watanabe, T., 2008. Block sampler and posterior mode estimation for asymmetric stochastic volatility models. Comput. Stat. Data Anal. 52-6, 2892–2910.

Patton, A.J., 2011. Volatility forecast comparison using imperfect volatility proxies. J. Econom. 160, 246–256.

Philipov, A., Glickman, M.E., 2006. Factor multivariate stochastic volatility via wishart processes. Econom. Rev. 25, 311–334.

Pitt, M.K., Shephard, N., 2003. Time Varying Covariance: A Factor Stochastic Volatility Approach (With Discussion). Oxford University Press, Oxford.

Pourahmadi, M., 1999. Joint mean-variance models with applications to longitudianl data: Unconstrained parametrisation. Biometrika 86, 677–690.

Shephard, N., Pitt, M.K., 1997. Likelihood analysis of non-gaussian measurement time series. Biometrika 84, 653–667.

Shirota, S., Hizu, T., Omori, Y., 2014. Realized stochastic volatility with leverage and long memory. Comput. Stat. Data Anal. 76, 618–641.

Takahashi, M., Omori, Y., Watanabe, T., 2009. Estimating stochastic volatility models using daily returns and realized volatility simultaneously. Comput. Stat. Data Anal. 53-6, 2404–2426.

Trojan, S., 2015. Essays on Multivariate Stochastic Volatility Models. Universität St. Gallen Thesis.

Venter, J.H., de Jongh, P.J., 2014. Extended stochastic volatility models incorporating realized measures. Comput. Stat. Data Anal. 76, 687–707.

Watanabe, T., Omori, Y., 2004. A multi-move sampler for estimating non-gaussian time series models: Comments on Sephard and Pitt (1997). Biometrika 91, 246–248.

Windle, J., Carvalho, C.M., 2014. A tractable state-space model for symmetric positive-definite matrices. Bayesian Anal. 9, 759–792.

Zheng, T., Song, T., 2014. A realized stochastic volatility model with box-cox transformation. J. Bus. Econ. Stat. 32, 593–605.